



Characterisation of human ERAL1 as an essential mitochondrial protein

Sven Dennerlein B.Sc.

Thesis submitted to Newcastle University in candidature for
the degree of Doctor of Philosophy

Newcastle University
Faculty of Medical Sciences
Institute for Ageing and Health
Mitochondrial Research Group
December 2010

Abstract

Mitochondria are cellular organelles that are present in all nucleated eukaryotic cells and contain their own genome (mtDNA). Mitochondrial DNA encodes beside 13 polypeptides and 22 tRNAs, 2 ribosomal RNAs. All mtDNA encoded proteins are synthesized within the mitochondrial matrix and essential parts of intra membrane multi-enzyme complexes, involved in oxidative phosphorylation. Mitochondrial protein synthesis is therefore essential for life. This process, however, is still poorly understood. Around 100 mitoribosomal proteins, initiation and elongations factors are involved in mitochondrial translation but the exact mechanisms of how the mitochondrial 55S monosome and the constituted subunits assemble remain obscure.

In an attempt to identify factors that play a role in mitoribosome assembly, proteomic analyses of affinity purified complexes using mtRRF were performed (Rorbach *et al.*, 2008). One identified protein was ERAL1, a KH domain containing GTPase with sequence similarity to Era, a eubacterial protein involved in maturation of the 16S-*rRNA*. SiRNA mediated ERAL1 depletion experiments in human cell lines were established and used to investigate the molecular function of the protein. As data in this thesis show, ERAL1 is a mitochondrial protein and is essential for mammalian cells. ERAL1 acts in mitochondria as a 12S-*rRNA* chaperone via binding at a conserved stem loop structure close to the 3' terminus of the 12S-rRNA and loss affects the assembly of the small mitoribosomal subunit. Depletion of ERAL1 causes its major growth phenotype, partly by inducing apoptosis. Thus the mitochondrial oxidative phosphorylation machinery is not affected during ERAL1 depletion.

ERAL1 is therefore an essential protein in eukaryotic cells, involved in 12S-*rRNA* maintenance.

Acknowledgments

First of all I want to say thanks to Dr. Zosia Chrzanowska-Lightowlers and Prof. RN Lightowlers for the possibility to do my PhD studies in the Mitochondrial Research Group. Their personal enthusiasm and permanent help during the last 3 years enabled me to attain this thesis. Especially the help and advice of Prof. RN Lightowlers during the thesis writing was inestimable. I also thank Prof. Doug Turnbull for believing in me to do this PhD studies.

Various people were involved in the project. I want to thank our collaborators in Nijmegen, Ing. Johannes Wessels and Prof. Jan Smeitink from the Nijmegen Centre for Mitochondrial Disorders in the Netherlands, for the excellent cooperation and work in the LC/MS mass spectroscopy. Dr. Rebecca Steward and Mr. Ian Dimmik for helping me a lot with the FACS analysis.

I would like to thank all members of the MRG group. Thanks Richard, for your advice with the RNA work. To Mateusz, many thanks for helping me during the practical training and for the helpful tips during the project. Helen, thank you for the help with the high-resolution northern and for providing me so many probes. Thank you Agata for keep going with the CLIP assay. Many thanks also to you Geoff for helping so often with sequencing. I also want to say thanks to you Ola, it was a pleasure to work with you.

To all other people in the lab, past and present, that encouraged me during the project: Martin, Paul...

The biggest thanks goes to Rica, my mum, Willi and Carola to get with me through the last 4 years with all the ups and downs so far from home.

Author's Declaration

I certify that for a degree or other qualification in the Newcastle University and any other institution neither I nor any other person had previously included the presented material in this thesis. All presented work is my own independent contribution, unless stated otherwise.

This work was carried out in the Newcastle University, Institute for Aging and Health, Mitochondrial Research Group under supervision of Prof. Doug M. Turnbull and Prof. Robert N Lightowlers, between October 2007 and November 2010.

Sven Dennerlein

Table of contents

Chapter 1 Introduction

1.1	Origins of mitochondria.....	2
1.2	Structure of mitochondria.....	2
1.3	The role of mitochondria in energy metabolism.....	5
1.4	ROS and mitochondria.....	9
1.5	Mitochondria and apoptosis.....	11
1.6	A small circle, important for life – mtDNA.....	13
1.7	Transcription of mtDNA.....	16
1.8	Mitochondrial RNA turnover.....	19
1.9	Protein synthesis in human mitochondria.....	20
	1.9.1 Translation initiation.....	22
	1.9.2 Translation elongation.....	24
	1.9.3 Translation termination and ribosome recycling.....	25
1.10	An overview of special features of the small mitoribosomal subunit.....	27
	1.10.1 Proteins of the mitochondrial 28S mt-SSU.....	27
	1.10.2 The ribosomal RNA of the 28S mt-SSU.....	28
	1.10.3 Human diseases associated with the 28S mt-SSU and its assembly.....	30
1.11	The prokaryotic protein Era.....	31
1.12	The eukaryotic ERAL1 protein.....	33
1.13	KH domains in prokaryotes and eukaryotes.....	35
1.14	Aims of the project.....	36

Chapter 2 Materials and methods

2.1	Materials.....	37
2.1.1	Bacterial strains.....	37
2.1.2	Plasmids.....	37
2.1.3	Eukaryotic cell lines.....	38
2.2	Methods.....	39
2.2.1	Tissue culture.....	39
2.2.1.1	Cell culture and maintenance.....	39
2.2.1.2	Cell storage.....	39
2.2.1.3	Cell counting.....	40
2.2.1.4	Mycoplasma testing.....	40
2.2.1.5	siRNA transfection.....	40
2.2.1.5 A	Reverse transfection of siRNA molecules.....	42
2.2.1.5 B	Forward transfection of siRNA molecules.....	42
2.2.1.6	Transfection of DNA in HEK293 Flp-In™ T-REx™ cells.....	43
2.2.2	Bacterial culture.....	45
2.2.2.1	Transformation of chemical competent cells.....	45
2.2.2.2	Colony screening.....	45
2.2.2.3	Isolation of plasmid DNA from bacteria.....	46
2.2.3	DNA manipulation.....	47
2.2.3.1	DNA extraction from human cell lines.....	47
2.2.3.2	Amplification of DNA by polymerase chain reaction (PCR)..	47
2.2.3.3	Purification of PCR products.....	48
2.2.3.4	Phenol/chloroform extraction and EtOH precipitation.....	48
2.2.3.5	Agarose gel electrophoresis.....	49
2.2.3.6	Enzymatic restriction of DNA.....	49
2.2.3.7	Dephosphorylation of plasmid DNA.....	50
2.2.3.8	Ligation reaction.....	50
2.2.3.9	DNA quantification.....	50
2.2.3.10	DNA sequencing.....	50
2.2.3.11	Southern blot analysis.....	51
2.2.4	RNA manipulation.....	53
2.2.4.1	RNA isolation from human cell lines.....	53

2.2.4.2 RNA isolation from liquid samples.....	54
2.2.4.3 Northern blot analysis.....	54
2.2.4.4 High resolution (HR) northern blot analysis of mt-tRNA.....	57
2.2.4.5 Reverse transcription.....	59
2.2.4.6 Real time PCR.....	59
2.2.5 Protein manipulation techniques.....	61
2.2.5.1 Preparation of protein lysates from cultured cells.....	61
2.2.5.2 Isolation of mitochondrial proteins.....	61
2.2.5.3 Bradford assay.....	62
2.2.5.4 SDS polyacrylamide gel electrophoresis (SDS-PAGE).....	63
2.2.5.5 Immunoblotting (Western Blot).....	64
2.2.5.6 Isokinetic sucrose gradient analyses.....	66
2.2.5.7 Coomassie Blue staining of polyacrylamide gels.....	67
2.2.5.8 Silver staining.....	67
2.2.5.9 SimplyBlue™ Safe Stain (Invitrogen, LC6060).....	68
2.2.5.10 <i>In vivo</i> metabolic radiolabelling of mitochondrial encoded proteins.....	68
2.2.5.11 FLAG-immunoprecipitation (IP) experiments.....	69
2.2.6 Cross Linking Immunoprecipitation assay (CLIP).....	72
2.2.7 Measuring respiration rate via oxygen consumption.....	73
2.2.8 Flow cytometric analysis.....	74
2.9 Phosphorimaging and statistical analysis.....	76
Chapter 3 <u>ERAL1 is a mitochondrial protein, involved in 28S mt-SSU assembly</u>	
3.1 ERAL1 is a mitochondrial protein.....	79
3.2 ERAL1 is an essential mitochondrial protein.....	80
3.3 ERAL1 interacts with the mitochondrial gene expression machinery.....	85
3.4 ERAL1 associates with the small mitochondrial ribosomal subunit.....	89
3.5 Depletion of ERAL1 causes loss of <i>de novo</i> 28S mt-SSU.....	92
3.6 Discussion.....	99

Chapter 4	<u>ERAL1 is involved in 12S-rRNA maintenance</u>	
4.1	Depletion of ERAL1 leads to increased levels of mt-mRNA.....	105
4.2	Mitochondria RNA levels increase in lighter sucrose gradient fractions.....	109
4.3	Depletion of ERAL1 leads to a minor loss in the stability of mt-RNA.....	116
4.4	ERAL1 depletion affects mt-tRNA.....	121
4.5	The stability of mt-tRNAs is not affected by ERAL1 depletion.....	125
4.6	Depletion of ERAL1 does not affect mt-mRNA stability in absence of 28S mt-SSU.....	127
4.7	Depletion of ERAL1 does not alter mtDNA level.....	131
4.8	ERAL1 acts as 12S-rRNA chaperone.....	133
4.9	Discussion.....	137
Chapter 5	<u>Loss of ERAL1 induces apoptosis</u>	
5.1	Depletion of ERAL causes a minor mitochondrial translation defect in HEK293-T cells.....	145
5.2	Proteins of the oxidative phosphorylation machinery are not affected by ERAL1 depletion.....	148
5.3	Depletion of ERAL1 increases the mitochondrial membrane potential.....	150
5.4	Depletion of ERAL1 does not elevate ROS.....	152
5.5	Loss of ERAL1 does not affect mitochondrial mass.....	154
5.6	Depletion of ERAL1 does not alter the cell cycle.....	156
5.7	Loss of ERAL1 induces apoptosis.....	159
5.8	Discussion.....	162
Chapter 6	<u>General Discussion and future aspects</u>	168
References.....		173
Appendix 1:	Identified proteins of the eluate from ERAL1-FLAG in comparison to mtLuc-FLAG during LC/MS mass spectroscopy.....	203
Appendix 2:	Identified sequences of RNA covalent bound to ERAL1 during CLIP assay.....	209

Appendix 3.1 Polarographic analysis of siRNA mediated ERAL1 depleted Hek293-T cells using the Oroborus-2k system.....	212
Appendix 3.2: Treatment of HEK293-T cells with FCCP.....	214
Appendix 3.3: MitoSOX™ measurements of Guf1.....	215
Publications.....	216

List of Figures

1.1	Electron microscopy image of a mitochondrion and 3D model.....	3
1.2	Schematic overview of the mitochondrial OXPHOS system in human mitochondria.....	6
1.3	Mitochondrial pathways of cellular apoptosis.....	11
1.4	Map of the human mitochondrial genome.....	14
1.5	The “ribomotor” loop model.....	18
1.6	Overview of the human mitochondrial protein synthesis.....	24
1.7	Structure of 16S-rRNA from <i>Thermus thermophilus</i> and bovine 12S-rRNA.....	29
1.8	3D structure of the <i>Aquifex aeolicus</i> Era protein with 16S-rRNA.....	32
1.9	Sequence alignment of Era and ERAL1 from <i>Escherichia coli</i> , <i>Aquifex aeolicus</i> , <i>Rickettsia prowazekii</i> <i>Mus musculus</i> , <i>Homo sapiens</i>	34
1.10	Typ II KH domain.....	35
2.1	Schematically overview of siRNA mediated mRNA degradation.....	41
2.2	Transfection of the ERAL1 gene in Flp-In™ T-Rex™ HEK293-T cells.....	44
2.3	Immunoprecipitation of FLAG-tagged proteins with covalent bound RNA...	71
2.4	Cross linking with immunoprecipitation.....	72
3.1	ERAL1 is localised and imported into human mitochondria.....	80
3.2	SiRNA mediated depletion of ERAL1 in HeLa and HEK293-T cells.....	81
3.3	Growth analysis of HeLa or HEK293-T cells within siRNA mediated depletion of ERAL1 and si-NT control.....	82
3.4	Depletion of ERAL1 using siRNA si-UTR and simultaneous expression of ERAL1-FLAG.....	83
3.5	Cell count of 143B.206-rho ⁰ or 143B rho ⁺ parental cells after 3 days treatment with si-UTR, si-ORF1 and si-NT.....	84
3.6	Eluates from ERAL1-FLAG immunoprecipitations contain mitoribosomal proteins.....	86
3.7	LC/MS mass spectroscopy analysis of affinity purified mitoribosomal proteins with ERAL1-FLAG.....	88
3.8	Isokinetic gradient analysis of mitoribosomal proteins in HeLa or HEK293-T cells.....	90

3.9	Isokinetic sucrose gradient analysis of eluate from the MRPS27-FLAG immunoprecipitation.....	91
3.10	Isokinetic sucrose gradient analyses of siRNA depleted ERAL1 HEK293-T cells.....	94
3.11	Effects on <i>de novo</i> formation of mitoribosomal complexes during ERAL1 depletion.....	97
3.12	Effects of ERAL1 depletion in human cell lines.....	104
4.1	Northern blot analysis of mt-RNA after 3 and 4 days ERAL1 depletion in HeLa cells.....	107
4.2	Northern blot analysis of mt-RNA after 3 and 4 days ERAL1 depletion in HEK293-T cells.....	108
4.3	Mt-RNA analysis of isokinetic sucrose gradient fractions post ERAL1 depletion in HEK293-T cells.....	111
4.4	Graphical presentation of RNA distribution in isokinetic sucrose gradient analysis after ERAL1 depletion.....	114
4.5	Northern blot analysis of EtBr treatment of HEK293-T cells after ERAL1 depletion.....	118
4.6	High-resolution northern blot analysis of mt-tRNAs post ERAL1 depletion after 3 and 4 days in HeLa cells.....	122
4.7	High-resolution northern blot analysis post ERAL1 depletion in HEK293-T cells.....	124
4.8	High-resolution northern blot analysis of EtBr treated HEK293-T cells post ERAL1 depletion.....	126
4.9	Northern blot analysis post over expression of mtPARN in HEK293-T cells and simultaneously depletion of ERAL1.....	130
4.10	Southern blot analysis of mtDNA after ERAL1 depletion.....	132
4.11	Region of <i>12S-rRNA</i> bound to ERAL1.....	136
4.12	Effects of ERAL1 depletion in human cell lines (continued I).....	144
5.1	Metabolic labelling of mtDNA encoded polypeptides.....	147
5.2	Western blot analysis of cell lysate from ERAL1 depleted HeLa and HEK293-T cells.....	149
5.3	Quantification of the mitochondrial membrane potential after ERAL1 depletion in HEK293-T cells.....	151
5.4	ROS is not accumulated in ERAL1 depleted HEK293-T cells.....	153
5.5	Flow cytometric analysis of cardiolipin staining with NAO.....	155

5.6	Flow cytometric cell cycle analysis of ERAL1 depleted and si-NT transfected HEK293-T cells.....	157
5.7	Graphed quantification of cell cycle analysis.....	158
5.8	Debris analysis of ERAL1 depleted and si-NT transfected HEK293-T cells.....	159
5.9	Apoptosis measurements of ERAL1 depleted and si-NT control cells.....	160
5.10	Quantification of apoptotic cells in ERAL1 depleted HEK293-T cells.....	161
5.11	Polarographic analysis of siRNA mediated ERAL1 depleted Hek293-T cells using the Oroborus-2k system.....	212
5.11	FCCP treatment of HEK293-T un-transfected cells.....	214
5.12	ROS accumulation during Guf1 depletion in HEK293-T cells.....	215
6.1	Effects of ERAL1 depletion in human cell lines (continued II).....	169

List of Tables

2.1	Bacterial strains with genotype and application.....	37
2.2	Used vectors with application.....	37
2.3	Sense-sequences of used siRNA nucleotides for ERAL1 depletion.....	43
2.4	Parameters of PCR reactions.....	48
2.5	Oligonucleotides used for PCR reactions to clone ERAL1-FLAG.....	48
2.6	Oligonucleotides used for sequencing reactions.....	51
2.7	Oligonucleotides used for PCR amplification of southern- and northern probes.....	55
2.8	Oligonucleotides used to amplification mt-tRNAs and 5S-rRNA regions...	58
2.9	Parameters of a real time PCR reaction.....	60
2.10	Oligonucleotides used for real time PCR.....	60
2.11	Components of polyacrylamide gels.....	63
2.12	Antibodies used for western blotting.....	65
4.1	Calculated half-life of mt-RNA in control and ERAL1 depleted cells.....	120
4.2	RT-PCR analysis of immunoprecipitations of UV irradiated ERAL1-FLAG..	134

Abbreviations

<i>A. aquifecs</i>	<i>Aquafix aquifecs</i>
AA	Amino acid
AB	Antibody
Amp	Ampicillin
A-site	Aminoacyl-tRNA ribosomal binding site
APS	Ammonium peroxidisulphate
ATP	Adenosine triphosphate
bp	Base pair(s)
c	Cytosine
CL	Cell lysate
CLIP	Crosslinking immunoprecipitation
CMV	Cytomegalivirus
cpm	Counts per minute
COX	Cytochrome c oxidase
C-terminus	Carboxyl-terminus
Da	Dalton
DAPI	4'-6'-Diamidino-2-phenylindole
ddH ₂ O	Distilled deionised water
D-loop	Displacement loop
DMEM	Dulbecco's modified Eagle's medium
DMSO	Dimethylsulphoxide
DNA	Deoxyribonucleotide acid
DNase	Deoxyribonuclease
dNTP	Deoxynucleotide triphosphate
dsDNA	Double strand DNA
DTT	Dithiothreitol

<i>E. coli</i>	<i>Escherichia coli</i>
EDTA	Ethylenediaminetetraacetic acid
EF-G	Elongation factor G
EF-Tu	Elongation factor Tu
EF-Ts	Elongation factor Ts
EGTA	Ethylene glycol tetra-acetic acid
EM	Electron microscopy
EMEM	Eagle's modified essential medium
EMPAI	Experimental modified Protein Abundance Index
ER	Endoplasmic reticulum
E-site	Exit side within the ribosome
EtBr	Ethidium bromide
EtOH	Ethanol
FAD	Flavin-adenine dinucleotide
FBS	Foetal bovine serum
FCCP	Trifluorocarbonylcyanide phenylhydrazone
FITC	Fluorescein isothiocyanate
fMet	Formyl-methionine
FMN	Flavine mononucleotide
FRT	Flp-recombination-target
g	Relative centrifugal acceleration
G	Guanine
Gal	Galactose
GDP	Guanine diphosphate
GFP	Green fluorescent protein
h	Hour
HEK293-T	Human embryonic kidney cells
HeLa	Human cervical cancer carcinoma cells from <u>H</u> enrietta <u>L</u> acks
<i>H. sapiens</i>	<i>Homo sapiens</i>

HSP	Heavy strand promoter
H-strand	Heavy strand
IF(s)	Initiation factor(s)
IgG	Immunoglobulin tyoe G
IP	Immuniprecipitation
JC1	5,5',6,6'-tetrachloro-1,1',3,3'-tetraethylbenzimi-dazolyIcarbocyanine iodide
kb	Kilobase(s)
KCl	Potassium chloride
kDa	Kilo Dalton
KOD	DNA polymerase from <i>Thermococcus kodakaraensis</i>
LB	Luria-Bertani bacterial medium
LC MS/MS	Liquid chromatography - tandem mass spectrometry
LSP	Light strand promoter
L-strand	Light strand
LSU	Large ribosomal subunit
MgCl ₂	Magnesium chloride
MgSO ₄	Magnesium sulfate
min	Minute(s)
MOPS	4-Morpholine-propanesulfonic acid
mRNA	Messenger RNA
MRP(L/S)	Mitochondrial ribosomal protein (of the <u>l</u> arge/ <u>s</u> mall subunit)
mt	Mitochondrial
mtDNA	Mitochondrial DNA
mtPTP	Mitochondrial permeability transition pore
MW	Molecular weight
NaAc	Sodium acetate
NAD	Nicotine-amid dinucleotide
NADH+H ⁺	Reduced nicotinamide-adenine dinucleotide

NAO	10-n-nonyl-acridine orange
nDNA	Nuclear DNA
NP-40	Nonident-P40; octyl phenoxy-polyethoxy-ethanol
nt	Nucleotide
N-terminus	Amino-terminus
OD	Optical density
ORF	Open reading frame
Ori _H	Origin of heavy strand replication
Ori _L	Origin of light strand replication
OXPHOS	Oxidative phosphorylation
p	P-value
PABP	Poly(A) binding protein
PAG(E)	Polyacrylamide gel (electrophoresis)
PAM	Presequence translocase-associated motor
PBS	Phosphate buffered saline
PCR	Polymerase chain reaction
PI-mix	Protease inhibitor cocktail
PMSF	Phenylmethanesulphonyl fluoride
PPR	Putative pentatricopeptide repeat
P-site	Peptidyl-tRNA site within the ribosome
PVDF	Polyvinylidene difluoride
q	Ubiquinone, coenzyme Q
RBP	RNA binding protein
RF(s)	Release factor(s)
RISC	RNA-induced silencing complex
RNase	Ribonuclease
RNA	Ribonucleotide acid
rRNA	Ribosomal ribonucleotide acid
ROS	Reactive oxygen species

rpm	Rounds per minute
RRF	Ribosome recycling factor
rRNA	Ribosomal RNA
RT	Reverse transcription
<i>S. cerevisiae</i>	<i>Saccharomyces cerevisiae</i>
SAM	Sorting and assembly machinery
s	Seconds
SDH	Succinate-dehydrogenase
SDS	Sodium dodecyl sulfate
siRNA	Small interfering RNA, silencing RNA
SN	Supernatant
SOC	Super optimal broth
SSC	Saline sodium citrate buffer
ssDNA	single stranded DNA
SSPE	Saline sodium phosphate buffer
SSU	Small ribosomal subunit
T	Thymine
TAE	Tris-acetate-EDTA buffer
<i>Taq</i>	<i>Thermus aquaticus</i>
TBE	Tris-borate-EDTA buffer
TBS	Tris buffered saline
TEMED	N,N,N',N'-Tetramethylethylenediamine
Tet	Tetracycline
TIM	Translocase of the inner mitochondrial membrane
TMRM	Tetramethyl rhodamine methyl ester
TOM	Translocase of the outer mitochondrial membrane
Tris	2-Amino-2-hydroxymethyl-propane-1,3-diol
Triton X-100	Polyethylene glycol p-(1,1,3,3-tetramethylbutyl)-phenyl ether
tRNA	Transfer RNA

TUNEL	Terminal deoxynucleotidyltransferase dUTP nick end labelling
Tween-20	Polyoxyethylene sorbitanmonolaurate
Unit	Enzyme activity (1U = 1 μ mol/ min)
U	Uracil
UTR	Untranslated region
UV	Ultraviolet light
vol	Volume
v:v	Volume:volume ratio
WT	wild type
w:v	Weight:volume ratio
xg	Relative centrifugal force

Chapter 1

Introduction

Chapter 1 Introduction

Mitochondria were discovered as separate unique cellular organelles, present in eukaryotic cells in the middle of the 19th century. In the 1950's the ultra-structure of mitochondria was discovered by high-resolution electron microscopy.

Soon afterwards mitochondria were identified as the main cellular energy suppliers by using transmembrane proton gradients generated from the final stage of oxidative metabolism of foodstuffs such as sugars and fats to produce ATP by forming phosphodiester bonds between ADP and inorganic phosphate. Our interest in understanding the functional mechanisms of mitochondria has increased rapidly during the last few decades and more cellular mechanisms such as ion-homeostasis, iron-sulfur-metabolism, apoptosis and cell cycle regulation have become associated with mitochondrial functions. In addition to housing key metabolic enzymes for oxidising fats and sugars, enzymes involved in other biological processes such as synthesis of cellular amino acids, phospholipids, pyrimidine biosynthesis and numerous biological cofactors are partly or entirely located in mitochondria. It soon became clear that alterations in mitochondrial functions are responsible for a range and variety of human diseases.

In contrast to other vertebrate organelles only the nucleus and mitochondria contain their own DNA. The human mitochondrial DNA (mtDNA) is a circular, covalently closed DNA molecule of 16,569 bp and encodes 37 genes whose products include 13 essential proteins of the mitochondrial oxidative phosphorylation machinery (OXPHOS). The remaining ~ 76 subunits of the OXPHOS machinery are nuclear encoded and must be imported into the organelle. Furthermore, all proteins that are involved in mitochondrial gene expression, including mtDNA replication, transcription and translation are encoded in the nucleus. A growing interest of the scientific world in mitochondrial gene expression and regulation during the last few years has shed light on some of the mechanisms involved in mitochondrial gene expression. However, a fundamental understanding of all aspects of the mitochondrial gene expression machinery is still elusive but is essential if we are trying to explain the role of mitochondrial dysfunction in numerous human diseases.

1.1 Origins of mitochondria

The human cell is a symbiosis of two forms of life where one is represented by the nucleus-cytosol and the other the mitochondrial component. It is now in general accepted that the mammalian cell we see today arose from a single endosymbiotic event 1 – 2 billion years ago (Margulis, 1970; Margulis, 1982; Gray, 1999; Gray *et al.*, 1999). The species that provided the nucleus-cytosol part emphasised its structure and took over many functions of the alpha-proteobacterial ancestor of the modern day mitochondrion, including the majority of genomic information (Wallace 1982; Gray *et al.*, 1999; Wallace, 2005). The human mitochondrion has retained only a small subset of 37 genes in the form of a circular DNA molecule with a size of ~ 16.5 kb (Anderson *et al.*, 1981) whose gene products are specialised in coupling respiration to the production of ATP, supplying the main energy for the cell.

Within the last decade, complete sequences of many mitochondrial genomes have been published including *Rickettsia prowazekii*, which is considered to be the closest ancestor of human mitochondria (Andersson *et al.*, 1998, Gray *et al.*, 1999).

1.2 Structure of mitochondria

The mitochondrial structure was visualised using high-resolution electron-microscopy from Palade (1952) and Sjöstrand (1956), both recognised mitochondria as multi-compartment organelles. In many cells, mitochondria form elongated tubules with a length of 1.0 – 2.0 μm and width of 0.2 – 1.0 μm that are changing size and shape or even moving along cytoskeletal structures (Bereiter-Hahn and Voth, 1994; Nunnari *et al.*, 1997). In fact, mitochondria are highly dynamic organelles within the cell and interact with other cell organelles like the endoplasmic reticulum (ER) (Mannella *et al.*, 1998; Mannella 2000; Pinton *et al.*, 2008) or even with each other being able to form large reticular networks during fusion or budding off during fission processes. The process of mitochondrial dynamics is clearly essential, and defects in components of the fusion process such as Mfn2 and OPA1 can cause diseases such as Charcot-Marie-Tooth 2A or dominant optic atrophy (reviewed by Hoppins *et al.*, 2007). Further, both proteins have been associated with apoptosis regulation in mammalian cells (Frezza *et al.*, 2006; Cipolat *et al.*, 2006; Karbowski and Youle, 2003).

The existence of two mitochondrial membranes (outer- and inner membrane) enables the formation of two aqueous compartments, denoted the intermembrane space and the mitochondrial matrix (Figure 1.1).

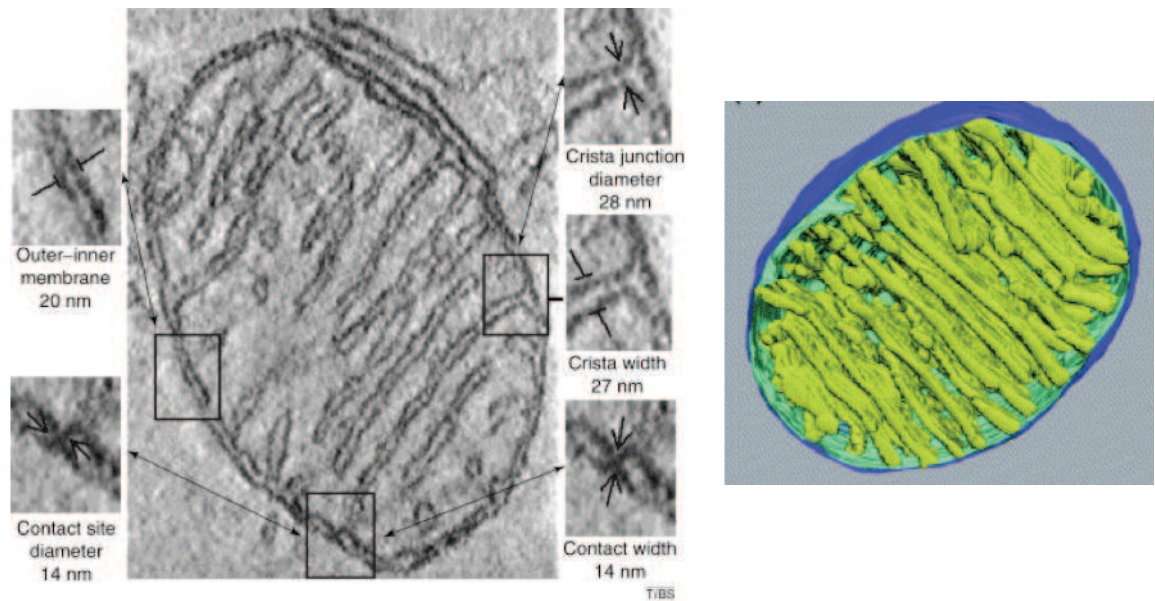


Figure 1.1: Electron microscopy image of a mitochondrion and 3D model. Left panel; Electron microscopy (EM) was used to visualise the mitochondrial structure of chicken cerebellar cells. Various structural features are enlarged, presented with size indications around the image and explained in the text. Right panel; 3D model calculated of EM images as presented in (A). Images were taken from Frey and Mannella (2000).

Both mitochondrial membranes harbour different enzymatic complexes and functions. The outer mitochondrial membrane carries the TOM complex, the main entry gate into mitochondria and also the SAM complex responsible for integration of proteins in the outer membrane (reviewed by Neupert and Herrmann, 2007 and Chacinska *et al.*, 2009). Further, the outer membrane is involved in fission and fusion processes, apoptotic regulation as well as in signaling pathways and is an interacting point with other cellular organelles such as the ER (reviewed by Ryan and Hoogenrad, 2007 and Frey and Mannella, 2000).

In contrast the inner mitochondrial membrane is protein rich and harbours oxidative phosphorylation complexes (OXPHOS), their assembly structures and protein degradation machineries such as membrane bound AAA-proteases (Nolden *et al.*, 2005). In mammals, five complexes are involved in OXPHOS (complex I – V). Additionally a large number of channel forming translocases are integrated in the inner mitochondrial membrane lipid bi-layer (Arco and Satrustegui, 2005) such as the TIM23-PAM complex (Chacinska *et al.*, 2005) facilitating further transport of proteins to the matrix or the TIM23^{SORT} complex (van der Laan *et al.*, 2006, Chacinska *et al.*, 2010), responsible for protein integration into the inner mitochondrial membrane, respectively.

The two mitochondrial membranes are separated from each other by the intermembrane space. This region is further divided into intermembrane boundary, a small space between outer and inner membrane, and cristae, which form long projections into the matrix (reviewed by Frey and Mannella, 2000). Further mobile redox-enzymes, cofactors and apoptosis associated factors are located in the intermembrane space (Koehler *et al.*, 2006; Webb *et al.*, 2006).

The mitochondrial matrix harbours the majority of mitochondrial proteins especially enzymes of metabolic processes as the TCA cycle or fatty-acid oxidation and can reach protein concentrations up to 560 mg/ml (reviewed by Ryan and Hoogenraad, 2007). Further all protein complexes involved in the mitochondrial gene expression machinery such as mtDNA replication and transcription, the mitochondrial ribosome, translational activators or repressor proteins and protein folding complexes are located in the matrix.

It has to be emphasised that mitochondrial compartments are functionally and physically connected to each other. Within the last few years efficient bioinformatic algorithms were developed to enable a more precise modeling of electron microscopy (EM) images. EM 3D tomography suggests a restriction of internal compartments. Small sections of the outer and inner membrane seem to be closer together than others originally denoted as “contact sides” (Hackenbrock, 1966) and are located at the inner boundary membrane close to the cristae base (Frey and Mannella, 2000). Further cristae are connected to the inner boundary membrane via cristae junctions (Perkins and Frey, 2000).

As reviewed by Westerhoff *et al.* (1988), these membrane connections enable mitochondria to control diffusion between internal compartments. Therefore, the mitochondrial membrane morphology might be able to regulate the redox-reactions involving release of cytochrome *c* from the intermembrane space during apoptosis. Thus, mitochondrial membranes are dynamic compartments, able to respond to alterations of metabolic conditions as already suggested in 1966 from Hackenbrock.

1.3 The role of mitochondria in energy metabolism

The main energy source of the cell is provided by the oxidative phosphorylation system, found within mitochondria. The respiratory chain in human mitochondria consists of four multi-subunits enzyme complexes, designated as NADH-coenzyme Q (CoQ) oxido-reductase or complex I; succinate-CoQ oxido-reductase (complex II), ubiquinol-cytochrome *c* oxido-reductase (complex III) and cytochrome *c* oxidase (complex IV). Additionally two electron carriers are involved, a lipophilic quinone, designated coenzyme Q (CoQ) or ubiquinone and one hydrophilic haem-protein, cytochrome *c*. This multi-enzyme system carries electrons from complex I and II to complex IV and the free energy released on electron transfer is used by complex I, III and IV to create an electrochemical proton gradient between the mitochondrial matrix and the intermembrane space. Electrons finally reduce molecular oxygen to water at complex IV. Protons in the intermembrane space flow back as a consequence of the proton gradient through the F_0 component of complex V which is embedded in the membrane, causing a rotation of the F_1 unit, leading to the synthesis of ATP from ADP. Complex I – IV in addition to complex V constitute the oxidative phosphorylation system (OXPHOS) (Figure 1.2).

The interest in mitochondrial oxidative phosphorylation over the last few decades, forced in part by association of defects in the OXPHOS machinery with human diseases, has been unable to completely explain these mechanisms at the molecular level although there are now crystallographic images of mammalian complexes II, III and IV, plus the F_1 component of complex V and very recently a structure of the complex I orthologue from the bacteria *Thermus thermophilus* published (Sun *et al.*, 2005; Iwata *et al.*, 1998; Tsukihara *et al.*, 1996; Abrahams *et al.*, 1994; Efremov *et al.*, 2010). However, using new methods development such as high-resolution X-ray crystallography or Blue Native Polyacrylamide Gel Electrophoresis (BN-PAGE) closer views of the biochemical functionality could be obtained.

The basic substrate to form finally ATP comes from the glycolytical pathway in the cytosol, where glucose a 6-carbon monosaccharide is oxidised to the monocarboxyl acid pyruvate. Pyruvate can be transported through the outer and inner mitochondrial membrane to the matrix side and reacts with coenzyme A to produce acetyl-CoA, which is further oxidised in the TCA cycle. Acetyl-CoA is also produced during fatty-acid metabolism (β -oxidation). During the TCA cycle three molecules of $\text{NADH} + \text{H}^+$ and one molecule FADH_2 are produced. These reduced cofactors donate electrons at complex I or II, respectively.

mtDNA	7	0	1	3	2
nDNA	39	4	10	10	14

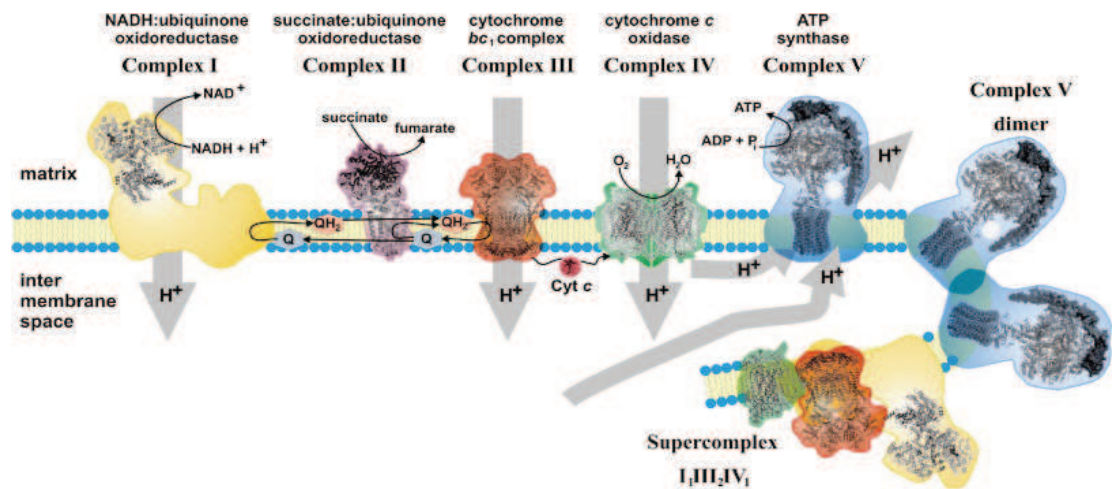


Figure 1.2: Schematic overview of the mitochondrial OXPHOS system in human mitochondria. Electrons fed into complex I from $\text{NADH} + \text{H}^+$ or into complex II from FADH_2 are transferred via coQ to complex III and are eventually transferred to molecular oxygen in complex IV to form water. Released energy during the electron transport is used by complex I, III and IV to pump protons from the mitochondrial matrix to the intermembrane space across the inner membrane (gray arrows), creating a proton gradient, which is used by complex V to generate ATP. Recent data suggest a clustering of several complexes in supercomplexes, indicated at the right. For a more detailed explanation of the OXPHOS machinery see text. Mitochondrial (mtDNA) and nuclear (nDNA) encoded proteins are marked above the image. The image is taken from Seelert *et al.* (2009).

NADH is the electron source for complex I, the largest and most complicated OXPHOS complex. The prokaryotic complex I contains 14 proteins (“core subunits”) (Weidner *et al.*, 1993). All these central subunits have orthologues in mammalian complex I (Gabaldon *et al.*, 2005) and seven of these proteins (ND1 – ND6 and ND4L) are encoded by the mtDNA (Carroll *et al.*, 2003, Ugalde *et al.*, 2004). Together with at least 39 additional proteins (Hincliffe and Sazanov, 2005; Scarpulla, 2008), these core subunits form a complex of ~ 1 MDa in mammals (Hirst *et al.*, 2003; Carroll *et al.*, 2003). The fine structure of the mammalian complex I is still elusive, however it has been suggested that complex I contains one hydrophilic peripheral arm facing the mitochondrial matrix and another hydrophobic membrane integrated module (containing ND1 – ND6 and ND4L), forming complex I in a “L-shaped boot” structure (Friedrich and Bottcher, 2004; Yagi and Matsuno-Yagi, 2003; Clason *et al.*, 2010; Morgan and Sazanow, 2008; Efremov *et al.*, 2010).

Electrons are fed into complex I on reduction of the NADH by FMN a non covalent bound flavin mononucleotide and are passed through the complex by a series of eight

redox-active iron-sulfur (Fe-S) clusters (Sazanov, 2007). The final electron acceptor is the lipophilic ubiquinone (CoQ), which is reduced to ubiquinol accepting two electrons. The transfer of two electrons is energetically coupled by pumping four protons from the matrix to the intermembrane space.

Complex II is entirely nuclear encoded and is composed of four subunits (reviewed from Rutter *et al.*, 2010). The complex is anchored in the inner mitochondrial membrane and contains two soluble factors SdhA, a flavoprotein and SdhB, an Fe-S cluster containing enzyme. These soluble proteins have succinate-dehydrogenase activity and catalyse oxidation of succinate to fumarate, producing FADH₂ in the TCA cycle. Electrons from FADH₂ are transported through the membrane integrated, Fe-S cluster containing proteins SdhC and SdhD, finally reducing CoQ.

The ubiquinol-cytochrome *c* oxidoreductase complex (complex III or *bc1* complex) is localised in the inner mitochondrial membrane and contains a highly conserved core unit comprised of the highly hydrophobic cytochrome *b* associated with the transmembrane proteins of the Rieske iron-sulfur protein and cytochrome *c*₁. It can only function as a dimer (Berry *et al.*, 2004). Electron transport through complex III is also known as the Q-cycle.

The reduction of ubiquinone to ubiquinol at complex I and II requires two electrons and protons. Ubiquinol is oxidised at the P centre of cytochrome *b* and is transferred through the Rieske protein and cytochrome *c*₁ to cytochrome *c*. The second oxidised electron of ubiquinol moves over the *bl* to the *bh* heme-centre and reduces ubiquinone to ubiquinol. A further ubiquinol oxidation at the P centre of cytochrome *b* donates the missing electron to further reduce ubiquinol to ubiquinol. The deprotonation of ubiquinol at the P centre and the protonation of ubiquinone at the N centre drives the transport of two protons through complex III to the intermembrane space, a movement that is further forced by the negative charged electrons through the *bl* and *bh* heme-centres.

Cytochrome *c* oxidase (complex IV) is also embedded in the inner mitochondrial membrane and harbours beside 10 nuclear encoded subunits three encoded by the mtDNA (COX1, COX2 and COX3). The X-ray structure of complex IV from bovine heart (Tsukihara *et al.*, 1996) identified these three proteins as the catalytic core of the enzyme. COX2, a two copper atom containing protein (CuA centre), acquires two electrons from reduced cytochrome *c* and passes them to COX1. The electrons are bound by COX1 at two cytochromes (*a* / *a*₃) and the copper B (CuB) centre. This reactive centre binds also molecular oxygen that functions as an electron acceptor and

is reduced to water. To reduce one molecule O_2 , four cytochrome c molecules have to be oxidised and the electrical force is used to pump four protons into the intermembrane space.

The ATP synthase or F_0F_1 -ATPase (reviewed by Yoshida *et al.*, 2001 and Fernández-Vizarra *et al.*, 2008) is a large complex of ~ 500 kDa and highly conserved through bacteria, plants and humans (Kanazawa *et al.*, 1981; Walker *et al.*, 1985). The complex contains 16 protein species in human, two encoded by the mtDNA (ATPase6 and ATPase8) that are arranged further into two large sub-complexes, a membrane-embedded F_0 part and a F_1 part (~ 380 kDa), facing the mitochondrial matrix. The two parts are connected by a central stalk that is formed by a subset of F_1 components (γ , δ , ϵ) and a peripheral stalk (or stator) containing OSCP, F6, b and d subunits. The F_1 sub-complex contains five kinds of subunits in stoichiometry $\alpha_3\beta_3\gamma_1\delta_1\epsilon_1$ and the F_0 contains eight different proteins (a, b, c, d, e, f, g and A6L).

Protons channeled through F_0 , force the central part of F_0 to rotate and trigger the rotation of $\gamma\epsilon$ -unit of F_1 . The rotation of the γ -subunit alternates, inducing other conformational changes, the structure of the β -subunits and forces ATP production. The active site of the matrix located F_1 component binds ADP and mitochondrial phosphate, forming a phosphodiester bound by further rotation of the complex. The synthesised ATP is transported to the cytosol through the ADP / ATP translocase in exchange with ADP.

Two different models proposed organisation of respiratory complexes in the inner mitochondrial membrane. The “random diffusion model” (Hackenbrock *et al.*, 1986) described OXPHOS complexes as randomly moving within the inner mitochondrial membrane and electrons transported between complexes by the mobile carrier ubiquinone / -ol and cytochrome c. The second model (solid model) suggests an organisation of complexes in larger structures to enable a quick transport of electrons through the OXPHOS machinery (reviewed by Lenaz and Genova, 2007).

Supercomplexes, multi-complex units of OXPHOS components, in cells were already predicted by Hatefi *et al.* (1961) for complexes I – III and from Yu *et al.* (1974) for complex II – III. More recently Schagger and Pfeiffer (2000) reported the existence of supercomplexes in yeast and mammalian cells. Blue Native Polyacrylamide Gel Electrophoreses (BN-PAGE) together with a mild digitonin-solubilisation of mitochondria was used to investigate interaction of different complexes. Complex I seem to be nearly entirely associated with other complexes (Schagger and Pfeiffer, 2001). Complex I and III form one supercomplex that is further assembled into two major supercomplexes (respirasomes) with different stoichiometries of complex IV

(I₁III₂IV₁ or I₁III₂IV₂). According to this model, the OXPHOS machinery is highly organised and enables a very efficient coupling between cellular respiration and ATP synthesis.

1.4 ROS and mitochondria

The term 'Reactive oxygen species (ROS)' (or indeed reactive nitrogen species, RNS) is generally used to describe O₂-derived free radical species in cells (reviewed by Circu and Aw, 2010). ROS exist in cells both as O₂-derived non-radical species - such as hydrogen peroxide (H₂O₂) and as damaging hydroxyl (HO[•]), peroxy (RO₂[•]) or alkoxy (RO[•]) radicals. However the most common radical is the superoxide anion (O₂^{•-}) and mitochondria are the major intracellular source of ROS. Although complex II was potentially associated with ROS production (Zhang *et al.*, 1998) it is mainly generated at the level of complex I and complex III of the respiratory chain (Brand, 2005). It has been postulated that as much as 0.2 - 2 % of the total mitochondrial consumed oxygen is regularly transformed to ROS (Boveris and Chance, 1973).

The biochemical mechanism of how ROS in form of superoxide (O₂^{•-}) is generated at complex I is not clear. It has been suggested that ROS is produced between the FMN and the rotenone-binding site (rotenone is a complex I inhibitor) or at one of the Fe-S centres (Herrero and Barja, 2000; Genova *et al.*, 2001).

ROS production at complex III is also controversial and still not fully understood but it is likely that superoxide (O₂^{•-}) is produced by involving unstable semiquinone, which may occasionally donate electrons directly to oxygen (Rich and Bonner, 1978). However, changes of physiological stages such as altering the membrane potential (Korshunov *et al.*, 1997) or the matrix pH (Lambert *et al.*, 2004) can trigger ROS production.

However, the OXPHOS machinery is by far not the only source of mitochondrial ROS. To date ~10 other potentially ROS generating mitochondrial systems have been described, distributed over all mitochondrial and cellular compartments (reviewed Andreyev *et al.*, 2005).

The outer membrane protein cytochrome *b5* reductase oxidises cytosolic NAD(P)H and reduces cytochrome *b5*, naturally producing superoxide (O₂^{•-}) at relatively high rates (Whatly *et al.*, 1998). At the outer surface of the inner mitochondrial membrane ROS has been reported to be produced in the form of H₂O₂ by glycerol-3-phosphate dehydrogenase in mouse (Kwong and Sohal, 1998) as well as in *Drosophila melanogaster* (Miwa *et al.*, 2004). Other ROS producers are the TCA cycle enzyme complexes such as aconitase, producing hydroxyl radicals (HO[•]) (Vasquez-Vivar *et al.*, 2000) in the mitochondrial matrix or enzyme complexes tightly associated with the

inner mitochondrial membrane like α -ketoglutarat dehydrogenase (α -KGDH) or pyruvate dehydrogenase are involved in generating superoxide ($O_2^{\cdot-}$) and hydrogen peroxide (H_2O_2) (Tretter and Adam-Vizi, 2004; Starkov *et al.*, 2004).

Several mechanisms have been developed during evolution to prevent damaging of cells by ROS. Cytochrome *c* previously described as a mobile component of the respiratory chain is capable of scavenging electrons directly from superoxide. The reduced cytochrome *c* is regenerated by complex IV (McCord and Fridovich, 1970).

Superoxide radicals ($O_2^{\cdot-}$) are the target of the mitochondrial manganese-containing superoxide dismutase (MnSOD). The enzyme is located inside mitochondria and dismutates superoxide radicals to H_2O_2 protecting Fe-S cluster proteins (Gardner *et al.*, 1995). H_2O_2 *per se* is also toxic for cells and has to be detoxified by other enzymes.

Catalase converts H_2O_2 in O_2 and H_2O . However, the removal of H_2O_2 by catalase is believed to be insignificant in comparison to glutathione peroxidase (Antunes *et al.*, 2002). The enzyme is ubiquitously expressed in tissues (Lenzen *et al.*, 1996) and was detected in different cellular compartments, including mitochondria. Potentially, glutathione peroxidase is the main cellular ROS-defending component, however, data from knock-out mice suggested a less essential role (Spector *et al.*, 1996; Cheng *et al.*, 1997; Ho *et al.*, 1997; Cheng *et al.*, 1998;).

Although the existence of ROS in cells was often thought to be only damaging, recent evidence has shown that mitochondrial derived ROS plays an essential role in several cellular signaling pathways. ROS has been associated with signals involved in the cell cycle, cell proliferation, metalloproteinase function, oxygen sensing, protein kinases, phosphatases, transcription factors and apoptosis (reviewed by Brooks *et al.*, 2004).

However, a chronic exposure to free radicals can damage different mitochondrial components. Superoxide radicals are dismutated to H_2O_2 by the MnSOD. H_2O_2 , in the presence of metal-ions, can be converted to the highly reactive hydroxyl radicals (HO^{\cdot}) via Fenton and/or Haber-Weiss reaction. ROS-mediated oxidative damage can affect most cellular component such as proteins, lipids or nucleic acids potentially contributed to the ageing process (Wei and Lee, 2002).

1.5 Mitochondria and apoptosis

In contrast to single-cellular organisms multi-cellular organisms have developed a self-demise mechanism, apoptosis. The destruction of infected, damaged or unwanted cells is necessary to ensure survival of healthy cells. The programmed cell death in human cells is divided in two main pathways, the extrinsic, mitochondrial independent pathway and the intrinsic. The apoptosis stimulation through the intrinsic pathway by ROS or mtDNA damage promotes mitochondrial permeability transition (PT) by forming a pore, reported as the point-of-no-return (Kroemer *et al.*, 1995). The PT-pore spans both mitochondrial membranes and includes the voltage-dependent anion channel (VDAC), the adenine translocase (ANT) and the only permanent component and modulator cyclophilin D (Bains *et al.*, 2005; Kokoszka *et al.*, 2004; Schinzel *et al.*, 2005).

Mitochondrial mediated apoptosis follows two independent pathways (Figure 1.4).

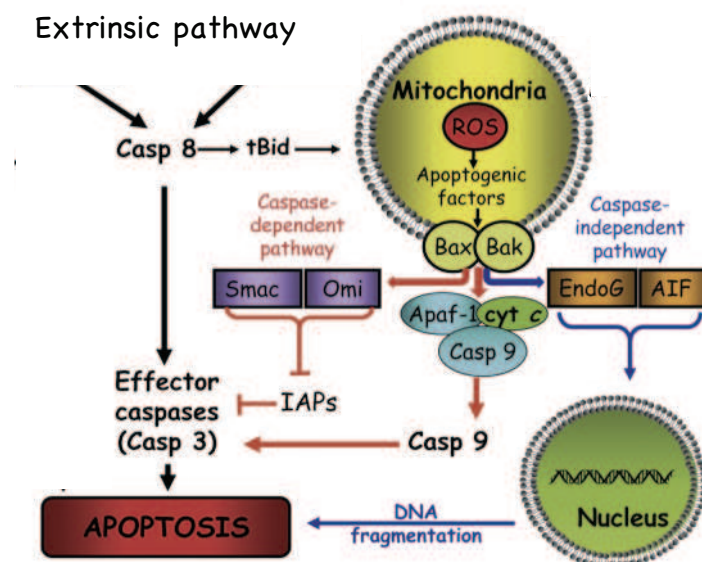


Figure 1.3: Mitochondrial pathways of cellular apoptosis. Intramitochondrial stimuli (e.g. ROS) activate the release of proapoptotic proteins by permeabilisation of the outer mitochondrial membrane. In the cytosol the apoptosome complex is formed by cytochrome c and Apaf-1. This complex recruits and activates pro-caspase-9, hence activating effector caspases (e.g. caspase-3) and initiating the final steps of apoptosis. To further enhance this pathway, complexes such as Smac/Diablo or Omi/HtrA2 inhibit anti-apoptotic proteins (IAPs). The caspase independent pathway is mediated by release of endonuclease G and the apoptosis inducing factor (AIF) from mitochondria. After reaching the cytosol both proteins translocate to the nucleus and mediate DNA fragmentation. The main regulatory factors are Bak and Bax protein containing complexes, for details see text. The image was adapted from Circu and Aw (2010).

During the caspase independent pathway, release of mitochondrial proteins to the cytosol such as AIF (apoptosis inducing factor) and endonuclease G, signals directly through the cytosol to the nucleus and induces nuclear chromatin condensation and DNA fragmentation (Susin *et al.*, 1999).

The second mitochondrial initiated pathway, denoted caspase dependent pathway, involves release of complexes such as Smac/Diablo and Omi/HtrA2 as well as cytochrome *c* (Liu *et al.*, 1996; Ryter *et al.*, 2007).

How cytochrome *c* exits the organelle is still under debate but two mechanisms have been proposed. First, the outer membrane bursts followed by matrix swelling and opening of a high-conductance channel in the inner membrane and loss of membrane potential (Bernardi, 1996). The second mechanism suggests a forced exit of cytochrome *c* by a yet unidentified pore in the outer membrane (Green and Reed, 1998). The PT-pore had been supposed to be involved in cytochrome *c* release (Simuzu *et al.*, 2001; Wang *et al.*, 2001); however, other studies reported that the PT-pore is not important (Basanez *et al.*, 1999). Recent studies suggested an involvement and remodeling of cristae junctions, regulated by Opa1 containing complexes (Frezza *et al.*, 2006; Yamaguchi *et al.*, 2008; Yamaguchi and Parkins, 2009). Opa1 is the mammalian counterpart of the yeast Mgm1 protein, localised to the inner membrane and involved in mitochondrial fusion (reviewed by Hoppins *et al.*, 2007). However, EM analysis of *Xenopus leavis* eggs showed that cytochrome *c* was released without any ruptures of the outer membrane (Kluck *et al.*, 1999). Further, the apoptotic mitochondria retained a membrane potential and continued to import proteins, strongly suggesting a controlled release of cytochrome *c* from the mitochondrial inter membrane space to the cytosol (von Ahsen *et al.*, 2000).

Cytochrome *c* forms the apoptosome with apoptotic protease activated factor 1 (Apaf-1) and recruits pro-caspase 9. This complex induces the cleavage of downstream effectors caspase-3 and -7. This simultaneously inhibits the Smac / Diablo - Omi / HtrA2 complex IAP (inhibitor of apoptosis protein), further enhancing caspase activation.

The main regulators of the mitochondrial apoptosis induced pathways are members of the Bcl-2 family, which can be divided in two classes: anti-apoptotic Bcl-2 family members (e.g. Bcl-XL, Bcl-w, Mcl-1, Bcl-Rambo) and pro-apoptotic proteins, such as Bax, Bak and Bok (Cory and Adams, 2002). A third group, BH3-family proteins (e.g. Puma, Noxa, Bid, Bad) inhibit Bcl-2 anti-apoptotic proteins and act as pro-apoptotic factors (Youle and Strasser, 2008).

However, the main intracellular target regulators of apoptosis seems to be Bak and Bax, because neither activation of BH3 proteins only nor suppression of Bcl-2 proteins is sufficient to trigger apoptosis (Zong *et al.*, 2001). Bax is a cytosolic monomer protein and translocates on apoptosis to mitochondria (Wolter *et al.*, 1997; Hsu *et al.*, 1997) forming oligomers (Antonsson *et al.*, 2001). Also the Bak protein oligomerises during apoptosis but is bound permanently as a monomer to the mitochondrial outer membrane (Griffiths *et al.*, 1999).

The intrinsic pathway can also be activated by cytosolic factors. A significant caspase 8 activation in the cytosol mediates a direct activation of caspase 3 and induces apoptosis. However, a low amount of activated caspase 8 cleaves the Bid protein and the activated tBid interacts with the Bax / Bak pro-apoptotic system, triggering apoptosis through the caspase dependent pathway (Barnhart *et al.*, 2003).

1.6 A small circle, important for life – mtDNA

Before the symbiosis of the proto-mitochondrion and the proto-host cell, both contained the genetic information sufficient for independent survival. The nucleus-cytosolic component subsumed most of the proto-mitochondrial functions during evolution and mitochondria to date have become highly specialised energy transducing organelles.

A few genes are still retained in mitochondria as the mtDNA (Nass and Nass, 1963) (Figure 1.4). The human mitochondrial DNA, in somatic cells is present in ~1000 – 10,000 copies (Smeitink *et al.*, 2001), is a covalently closed, double stranded circle of 16,569 bp (Anderson *et al.*, 1981). However, mtDNA contains a non-coding region, the D- or displacement loop and it is believed that the majority of mtDNA in this region is in a triplex formation at any time.

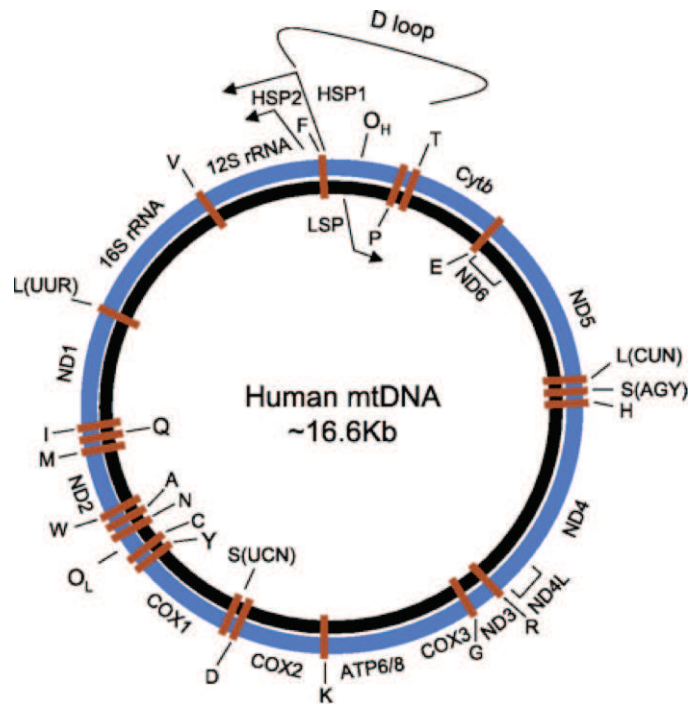


Figure 1.4: Map of the human mitochondrial genome. The human mitochondrial genome (mtDNA) has a size of ~16.6 kb. The two strands contain different amounts of G and C nucleotides and thus behave differently in caesium chloride gradients, denoted “heavy (H) strand” (blue) and “light (L) strand” (black). Thirty-seven genes are encoded in mtDNA, 13 proteins, 2 rRNA and 22 tRNAs (brown strings). In addition to the individual genes is the D-loop the only major non-coding region, present in a triplex structure. Although the H-strand origin (O_H) for mtDNA replication is placed in the D-loop region, the origin of the L-strand (O_L) is still under dispute and was suggested to be ~11 kb apart from O_H . Mitochondrial transcription starts at three independent promoters, two on the H-strand and one on the L-strand. The image was taken from Scarpulla (2008).

Mitochondrial DNA contains 37 genes, which encode 22 tRNAs, 2 ribosomal RNAs and 13 proteins, all essential subunits of the multiple enzyme complexes needed for oxidative phosphorylation (see 1.3) (Holt *et al.*, 1990; Hofhaus and Attardi, 1995). The two mtDNA strands, owing to differential nucleotide composition (G and C nucleotides) are denoted “heavy strand” (H-strand) and “light strand” (L-strand) dependent on their buoyant densities in caesium chloride gradients (Kasamatsu and Vinograd, 1974). The L-strand encodes 8 tRNAs and one polypeptide, ND6. All other mtDNA genes are encoded on the H-strand.

Human mtDNA lacks introns and genes are mostly separated by only a few nucleotides (Anderson *et al.*, 1981, Montoya *et al.*, 1982). Each polypeptide-encoding gene is flanked by at least one mt-tRNA encoding gene, described as the tRNA-punctuation

model (Ojala *et al.*, 1981). However, genes encoding ATPase6 and ATPase8 as well as ND4 and ND4L have overlapping open reading frames. Moreover, a number of genes lack the termination codon for the open reading frame, which is completed post-transcriptionally by poly(A)-addition (Ojala *et al.*, 1981).

The mtDNA contains a short (~ 1100 nt) triple-strand non-coding region, called the “displacement loop” or D-loop. Clayton (1982) proposed a model where the origin of the H-strand (O_H) is located in the D-loop region. The origin of the L-strand replication (O_L) was mapped ~ 11 kb apart from O_H (Shadel and Clayton, 1997; Shadel *et al.*, 2003). Recent studies by Brown *et al.* (2005) suggested multiple origins on the L-strand. Fusté *et al.* (2010) showed that the RNA polymerase functions as primase for DNA synthesis from O_{iL} and after about 25 nt is replaced by the mitochondrial polymerase POL γ . Therefore, the exact mechanism of L-strand replication remains elusive.

Several hypotheses have been proposed as why mitochondria still contain their own genomes (reviewed by Wallace, 2007).

Differences in the genetic code used by the cytosolic translation machinery in contrast to mitochondria were suggested to be a reason for retaining a separate mitochondrial genome (Osawa *et al.*, 1992; Doolittle, 1998; Wallace, 2005). The cytosolic stop codon UGA is decoded in mitochondria as tryptophan. Further, arginine is decoded in the cytosol from the triplet AGA and AGG. These codons are not recognised by an tRNA in the human mitochondrial DNA and are part of a back-translocation unit to invoke a -1 frameshift (Temperley *et al.*, 2010) at the termini of the two open reading frames of COX1 and ND6. Therefore mitochondria retain two stop codons, UAA and UAG in contrast to three of the cytosolic universal code. Further, the codon AUA is decoded in the cytosol as isoleucine and in mitochondria as methionine.

Another hypothesis stressed the functional importance of all mtDNA encoded proteins as evolutionary conserved core subunits of OXPHOS complexes. Therefore, they provide a scaffold in the inner mitochondrial membrane for the correct multi-enzyme complexes assembly. However, Wallace (2007) suggested that the mitochondrial import machinery would be efficient enough to assemble all complexes properly even if all components were to become nuclear encoded.

The third hypothesis argues that mtDNA encoded proteins are too hydrophobic to be translated in the cytosol or are mislocalised to other cell compartments such as the ER.

Spelbrink (2010) recently reviewed the organisation of mtDNA in dense packed nucleoid complexes. In mammals the first evidence of mtDNA organisation in nucleoid complexes was proposed by Satoh and Kuroiwa in 1991. Each nucleoid contains

Human ERAL1 is a mitochondrial RNA chaperone involved in the assembly of the 28S small mitochondrial ribosomal subunit

Sven DENNERLEIN, Agata ROZANSKA, Mateusz WYDRO¹, Zofia M. A. CHRZANOWSKA-LIGHTOWLERS² and Robert N. LIGHTOWLERS²

Mitochondrial Research Group, Institute for Ageing and Health, Newcastle University, Newcastle upon Tyne NE2 4HH, U.K.

The bacterial Ras-like protein Era has been reported previously to bind 16S rRNA within the 30S ribosomal subunit and to play a crucial role in ribosome assembly. An orthologue of this essential GTPase ERAL1 (Era G-protein-like 1) exists in higher eukaryotes and although its exact molecular function and cellular localization is unknown, its absence has been linked to apoptosis. In the present study we show that human ERAL1 is a mitochondrial protein important for the formation of the 28S small mitoribosomal subunit. We also show that ERAL1 binds *in vivo* to the rRNA component of the small subunit [12S mt (mitochondrial)-rRNA]. Bacterial Era associates with a 3' unstructured nonanucleotide immediately downstream of the terminal stem-loop (helix 45) of 16S rRNA. This site contains an AUCA sequence highly conserved across all domains of life, immediately upstream of the anti-Shine–Dalgarno sequence, which is conserved in bacteria.

Strikingly, this entire region is absent from 12S mt-rRNA. We have mapped the ERAL1-binding site to a 33 nucleotide section delineating the 3' terminal stem-loop region of 12S mt-rRNA. This loop contains two adenine residues that are reported to be dimethylated on mitoribosome maturation. Furthermore, and also in contrast with the bacterial orthologue, loss of ERAL1 leads to rapid decay of nascent 12S mt-rRNA, consistent with a role as a mitochondrial RNA chaperone. Finally, whereas depletion of ERAL1 leads to apoptosis, cell death occurs prior to any appreciable loss of mitochondrial protein synthesis or reduction in the stability of mitochondrial mRNA.

Key words: Era G-protein-like 1 (ERAL1), mitoribosome, ribosome assembly, rRNA, translation.

INTRODUCTION

Mammalian mitochondria possess their own genome, mtDNA (mitochondrial DNA), which encodes 13 proteins and all of the 24 RNA components necessary to drive intramitochondrial protein synthesis [1]. The remaining proteins required for this process, including all the protein components of the mitoribosome, are nuclear encoded, translated in the cytosol and imported into the organelle. Correct mtDNA expression is essential for all obligate aerobes, as these polypeptides constitute vital members of the protein complexes that couple oxidative phosphorylation. Protein synthesis is facilitated by the mitoribosome (i.e. the mitochondrial ribosome), whose assembly and molecular mechanisms are still largely uncharacterized. The mammalian 55S mitoribosome differs substantially from its 70S and 80S counterparts found in prokarya and the eukaryotic cytosol respectively [2,3]. Whereas it has minimized its rRNA components, it has extended its polypeptide constituents with the result that, although its overall mass is slightly greater than that of the bacterial ribosome (approx. 2.7 MDa), it has a decreased density. Thus the mt (mitochondrial)-SSU (small subunit) and mt-LSU (large subunit) are designated 28S and 39S respectively, generating a complete monosome of 55S. A highly purified bovine 55S mitoribosomal particle has been resolved to 13.5 Å (1 Å = 0.1 nm) by cryoelectron microscopy.

This indicates the positions of the shorter 12S and 16S mt-rRNA constituents relative to the 29 and 48 polypeptides within the mt-SSU and mt-LSU respectively [2]. It is possible, however, that a small number of less tightly associated *bona fide* members may have been lost during purification. Indeed, there is still some discussion as to the possible mitoribosomal association of a 5S rRNA species, which has been shown to be imported into mammalian mitochondria [4,5].

The assembly pathway of the mammalian mitoribosome is uncharacterized. It is believed that as many as 200 proteins are required to assemble the 80S ribosome in the yeast cytosol [6]. Bioinformatic analyses, however, suggest that mitoribosomal assembly may require only a minimal number of factors, more related to the situation in bacteria [7]. In an attempt to identify factors loosely associated with mitoribosomes, we recently performed a proteomic analysis of particles immunoprecipitated by the mtRRF (mitochondrial ribosome recycling factor) [8]. In addition to almost an entire set of mitoribosomal proteins, we identified nucleoid components and other proteins of unknown or diverse function. One of these proteins ERAL1 (Era G-protein-like 1), is the human orthologue of the *Escherichia coli* Ras-like protein Era [9]. In bacteria, this GTPase has been reported to be essential for cell division [10]. More recently, Era has been shown to bind via its C-terminal KH (K homology) domain

Abbreviations used: CLIP, cytoplasmic linker protein; COX, cyclo-oxygenase; DAP3, death-associated protein 3; ERAL1, Era G-protein-like 1; FBS, fetal bovine serum; GDH, glutamate dehydrogenase; HEK-293T, HEK (human embryonic kidney)-293 cells expressing the large T-antigen of SV40 (simian virus 40); HSP70, heat-shock protein 70; ICT1, immature colon carcinoma transcript 1; IP, immunoprecipitation; KH, K homology; LSU, large subunit; MEM, minimal essential medium; MGC, mammalian gene collection; MRP, mammalian ribosomal protein; mt, mitochondrial; MTND, mitochondrially encoded NADH dehydrogenase; NDUFA9, NADH dehydrogenase (ubiquinone) 1 α subcomplex 9; NDUF8, NADH dehydrogenase (ubiquinone) 1 β subcomplex 8; NEAA, non-essential amino acids; NT, non-targeting; RNP, ribonucleoprotein; ROS, reactive oxygen species; SD, Shine–Dalgarno; siRNA, small interfering RNA; SSU, small subunit; TFB1M, transcription factor B1, mitochondrial; UTR, untranslated region.

¹ Present address: Department of Plant Sciences, University of Cambridge, Downing Site, Downing Street, Cambridge CB2 3EA, U.K.

² Correspondence may be addressed to either of these authors (email z.chrzanowska-lightowlers@ncl.ac.uk or r.n.lightowlers@ncl.ac.uk).

to the 30S small ribosomal subunit near to the 3' terminus of the 16S rRNA [11,12]. These elegant X-ray diffraction and cryoelectron microscopy studies show Era bound either to an oligoribonucleotide or to the entire 30S subunit lacking ribosomal protein S1. Era both occludes the binding site for S1 and inhibits the interaction of the SD (Shine–Dalgarno) sequence of mRNAs with the anti-SD sequence at the 3' terminus of the mature 16S rRNA, each of which are required for translation initiation. Taken together, these results predict that Era plays an essential role in ribosome maturation and quality control. The few reports on the mammalian orthologue ERAL1, have suggested that it is a membrane-bound protein possibly associated with the endoplasmic reticulum [13] and that depletion led to growth arrest and apoptosis [14]. These latter functions were attributable to the conserved RNA-binding KH domain.

In the present study we show that ERAL1 is an essential mitochondrial protein. In a similar fashion to the bacterial orthologue, it associates mainly with the 28S mt-SSU where it acts as a chaperone for the 12S mt-rRNA, binding at the 3' terminal stem–loop region. Depletion of ERAL1 leads to 12S instability and a consequent loss of newly synthesized 28S subunits. We were able to confirm apoptosis, but intriguingly this occurred prior to any appreciable effect on mitochondrial protein synthesis or on the steady-state level of most mt-mRNAs.

EXPERIMENTAL

Cell culture

Human HeLa cells were propagated in Eagle's MEM (minimal essential medium; Sigma–Aldrich), supplemented with 1 × NEAA (non-essential amino acids), 10% (v/v) FBS (fetal bovine serum) and 2 mM L-glutamine, at 37°C under a 5% CO₂ humidified atmosphere. Osteosarcoma cells (143B.206 rho⁰) were provided by Professor R. Wiesner, Center for Molecular Medicine, University of Cologne, Germany, and were cultured in DMEM (Dulbecco's modified Eagle's medium) supplemented with 10% (v/v) FBS, 50 µg/ml uridine and 1 × NEAA. Flp-InTMT-RexTM-293 cells {HEK-293T [HEK (human embryonic kidney)-293 cells expressing the large T-antigen of SV40 (simian virus 40)]; Invitrogen} were grown in identical medium supplemented with 10 µg/ml Blasticidin S (Invitrogen). Post-transfection selection was effected with Hygromycin B (100 µg/ml). Growth curve analyses were performed in glucose medium.

Cell lysate, mitochondrial preparation and fractionation

Production of mitochondria and cell lysates were essentially as described in [15]. HEK-293T cells were homogenized on ice. Aggregates were removed by centrifugation at 400 g for 10 min at 4°C. Mitochondria were precipitated via centrifugation at 11 000 g for 10 min at 4°C. The post-mitochondrial supernatant was used for further analysis. Proteinase K treatment was carried out in a 50 µl volume of isolation buffer (10 mM Tris/HCl, pH 7.4, 0.6 M mannitol, 1 mM EGTA and 0.1% BSA), lacking BSA, containing 30 µg of freshly isolated mitochondria and the appropriate amount of proteinase K. Reactions were incubated on ice for 30 min, stopped by the addition of 2 mM PMSF, and mitochondria were then washed twice in 1 ml of the isolation buffer (without BSA) and re-suspended in the desired buffer. Where necessary, mitochondria were solubilized by the addition of 1% (v/v) Triton X-100.

Production of FLAG-tagged constructs, transfection and expression

The original human ERAL1 clone was obtained from the MGC (mammalian gene collection; clone 4893068; accession number BC019094). All constructs were prepared by PCR using the MGC clone as a template. Constructs to facilitate inducible expression of C-terminally FLAG-tagged ERAL1 were prepared by generating an amplicon using the following primers: forward 5'-ctctctg^{*gatccatg*}gctgccccagctg-3' and reverse 5'-ctctccg^{*gatcc*}ctactatctgctgctatccttgaatcctgaggagcttcacagag-3' (the ATG start codon is in bold; the BamHI restriction site is in italics). The original human MRPS26 (mammalian ribosomal protein S26) clone was obtained from MGC (clone 3051126; accession number BC013018). All constructs were prepared by PCR using the MGC clone as a template. Constructs to facilitate inducible expression of C-terminally FLAG-tagged MRPS26 were prepared by generating an amplicon using the following primers: forward 5'-tactatg^{*gatccaccatg*}ctacgctgctgag-3' and reverse 5'-atactactc^{*gagct*}actatctgctgctatccttgaatcggagctcctgctgttgg-3' (the ATG start codon is in bold; BamHI and XhoI restriction sites are in italics). Amplicons and pcDNA5/FRT/TO (Invitrogen) were digested with appropriate restriction enzymes and ligated. Fidelity and orientation were confirmed by sequence analysis. The human HEK-293T cells were transfected at ~50% confluency with the vectors pOG44 and pcDNA5/FRT/TO containing sequences of the genes to be expressed [FLAG-tagged ERAL1, MRPS27, ICT1 (immature colon carcinoma transcript 1)] as described previously [16].

Affinity purification and elution of FLAG-tagged polypeptides

For affinity purification either cell lysates or mitochondria from HEK-293T cells expressing FLAG-tagged derivatives were used. Cell lysates were prepared in lysis buffer [50 mM Tris/HCl, pH 7.4, 150 mM NaCl, 10 mM MgCl₂, 1 mM EDTA, 1% (v/v) Triton X-100, 1 × protease inhibitor cocktail (Roche) and 1 mM PMSF], and mitochondrial preparations were as described above. Mitochondrial preparations were treated with DNase I (0.5 units/mg of mitochondria) for 15 min at room temperature (22°C), and proteinase K (5 µg/mg of mitochondria) for 30 min at 4°C, reaction were then stopped by the addition by 1 mM PMSF. Pelleted mitochondria were washed (in homogenization buffer), digitonin-treated to remove the outer membrane (400 µg/mg of mitochondria), washed and finally resuspended in lysis buffer. Immunoprecipitation was effected with anti-FLAG M2-agarose affinity gel as recommended by the manufacturer (Sigma–Aldrich), followed by specific elution using 5 µg of 3 × FLAG peptide per 100 µl of elution buffer.

Isokinetic sucrose gradient analysis

Total cell lysates (0.5–0.7 mg in lysis buffer) or eluted IPs (immunoprecipitations) were loaded on to a linear sucrose gradient [1 ml, 10–30% (v/v)] in 50 mM Tris/HCl, pH 7.2, 10 mM magnesium acetate, 40 mM NH₄Cl, 0.1 M KCl, 1 mM PMSF and 50 µg/ml chloramphenicol, and with a Beckman OptimaTLX bench ultracentrifuge, using a TLS55 rotor at 39 000 rev./min for 135 min at 4°C. Fractions (100 µl) were collected and analysed by Western blot or by silver staining. For Western blot analysis, proteins from cell lysate, following sucrose-gradient separation, or after immunoprecipitation and elution, were separated by SDS/PAGE and transferred on to PVDF membranes as described in [8]. After binding of primary antibodies, visualization of specific proteins was facilitated with horseradish-peroxidase-conjugated secondary goat or mouse IgG (both Dako), using ECL

(enhanced chemiluminescence) Plus reagents (GE Healthcare) using a Storm 860 (GE Healthcare) PhosphorImager or by exposure to standard autoradiographic film. The following rabbit polyclonal antibodies were used: anti-ERAL1, -MRPS25, -MRPS18B (Protein Tech Group, catalogue numbers: 11478, 15277, 16139), anti-GDH (glutamate dehydrogenase) (in-house production), anti-MRPL3 (Abcam; catalogue number AB39268). Mouse monoclonal antibodies against: DAP3 (death-associated protein 3), HSP70 (heat-shock protein 70), MRPL12 (Abcam; catalogue numbers AB11928, AB2799, AB58334), β -actin (Sigma-Aldrich; catalogue number A1978), porin, COX2 (cyclo-oxygenase 2) (Invitrogen, catalogue numbers A33319A, A6404), NDUFA9 [NADH dehydrogenase (ubiquinone) 1 α subcomplex 9] and NDUFB8 [NADH dehydrogenase (ubiquinone) 1 β subcomplex 8] (Mitosciences U.S.A.; catalogue numbers MS111, MS105) were used. For silver staining polyacrylamide gels were fixed in 50% methanol for 1 h, followed by a 15 min incubation in staining solution [0.8% AgNO₃, 1.4% (v/v) NH₄OH and 0.075% NaOH], the washes of 5 min in nanopure distilled water, and then developed in 0.055% formaldehyde/0.005% citric acid and fixed in 45% methanol/10% acetic acid.

siRNA (small interfering RNA) constructs and transfection

Three sequences targeting ERAL1 were tested for efficiency of protein depletion: siORF1 (+702) 5'-GUGUCCUG-GUCAUGAACAA; siORF2 (+1096), 5'-GGAGGUGCC-UUACAAUGUA; siUTR (+1698), in the 3'-UTR (untranslated region), 5'-CCUUGAACUUGGAUAAGAA (starting nucleotide positions are relative to sequence NM_005702; sense sequence only given). Transfections were performed on 20% confluent HeLa cells with Oligofectamine (Invitrogen) in Opti-MEM-I medium (Gibco) with 0.2 μ M siRNA. Reverse transfections were performed as described in [17] on approx. 12 000 HEK-293T cells per cm² with LipofectamineTM RNAiMAX (Invitrogen) in Opti-MEM-I medium (10–33 nM siRNA). Custom and control non-targeting (NT; OR-0030-neg05) duplex siRNAs were purchased pre-annealed from Eurogentec.

Northern analysis

RNA was isolated with TRIzol[®] as recommended by the supplier (Invitrogen). Northern blots were performed as described in [18]. Briefly, aliquots of RNA (4 μ g) were electrophoresed through 1.2% (w/v) agarose under denaturing conditions and transferred on to GenescreenPlus membrane (NEN duPont) following the manufacturer's protocol. Radiolabelled probes were generated using random hexamers on PCR-generated templates corresponding to internal regions of the relevant genes.

Identification of oligoribonucleotides bound *in vivo* [CLIP (cytoplasmic linker protein) assays]

Assays were performed essentially as described in [19]. Briefly, cells expressing ERAL1 were grown to ~80% confluency in four 15 cm² plates, washed in PBS and UV-irradiated at 400 mJ/cm² in a Stratelinker (Stratagene). To ensure only short protected RNA species remained, cells were lysed, the bound RNP (ribonucleoprotein) was treated with RNase T1 and ERAL1 RNP was immunoprecipitated as above. Bound RNA was dephosphorylated and ligated to the 3' linker as described in [19]. To visualize the complex, the 5' termini were incubated with [γ -³²P]ATP (3000 Ci/mol, PerkinElmer)

and PNK (T4 polynucleotide kinase; New England Biolabs), separated by SDS/PAGE (10% Novex precast gels), transferred on to nitrocellulose (BA-85 Whatman) and subjected to autoradiography. For RNA isolation, bound RNP was cut from the nitrocellulose, protein was degraded with proteinase K and the RNA precipitated following phenol/chloroform extraction. Ligation of the 5' terminus, reverse transcription and PCR amplification were as described previously [19]. PCR products were ligated into pCR4-TOPO and inserts sequenced from individual clones (ABI 3130XL).

In vivo mitochondrial protein synthesis

Analysis of mitochondrial protein synthesis in cultured cells was performed as described previously [20] after addition of emetine and was pulsed with [³⁵S]methionine/cysteine for 30 min. Samples (50 μ g) were separated by SDS/PAGE (15% gels) and gels were exposed to PhosphorImage cassettes and visualized using ImageQuant software (GE Healthcare).

Analysis of apoptosis

The proportion of apoptotic cells was analysed using the APO-DIRECT kit (BD Biosciences) following the manufacturer's protocol. Labelling reactions were performed on 0.5×10^6 cells and FACS analysis performed on a three laser beam (633 nm, 488 nm and 405 nm) FACSCanto II (Becton Dickinson). Terminal deoxynucleotidyl transferase, used to detect the DNA strand breaks, was conjugated to FITC and measured from the excitation of the 488 nm laser and collected using a 530/30 bandpass PMT (photomultiplier tube) filter; 5000–10 000 cells were counted per analysis.

Statistical analysis

Where significance values are shown, *P* values were calculated using an unpaired Student's *t* test.

RESULTS

ERAL1 is a mitochondrial protein that associates with the small 28S subunit of the mitoribosome

To assess the cellular distribution of ERAL1, human HEK-293T cells were separated into cytosolic and mitochondrial fractions. Western blots revealed a strong co-localization with the crude mitochondrial fraction with no signal in the cytosol or nucleus (Figure 1A, left-hand panels). As it is formally possible that ERAL1 localizes to the mitochondrial periphery and remains associated with the mitochondrial outer membrane on subfractionation, isolated intact mitochondria were subjected to increasing amounts of proteinase K to remove co-purifying contaminants. As shown in Figure 1(A) (right-hand panel), ERAL1 remains resistant to the protease, similar to the mitochondrial matrix marker, GDH. Both proteins were digested after detergent solubilization of the organelles. A similar pattern was observed with subfractionated HeLa cells (results not shown). These results are consistent with ERAL1 being a mitochondrial protein, potentially within the mitochondrial matrix.

As Era, the bacterial orthologue of ERAL1, has been shown to play an important role in ribosome assembly, we next determined whether ERAL1 associates with mitoribosomal subunits. Following fractionation of HeLa cell lysates by sucrose gradients, a small population of ERAL1 was found in the lowest

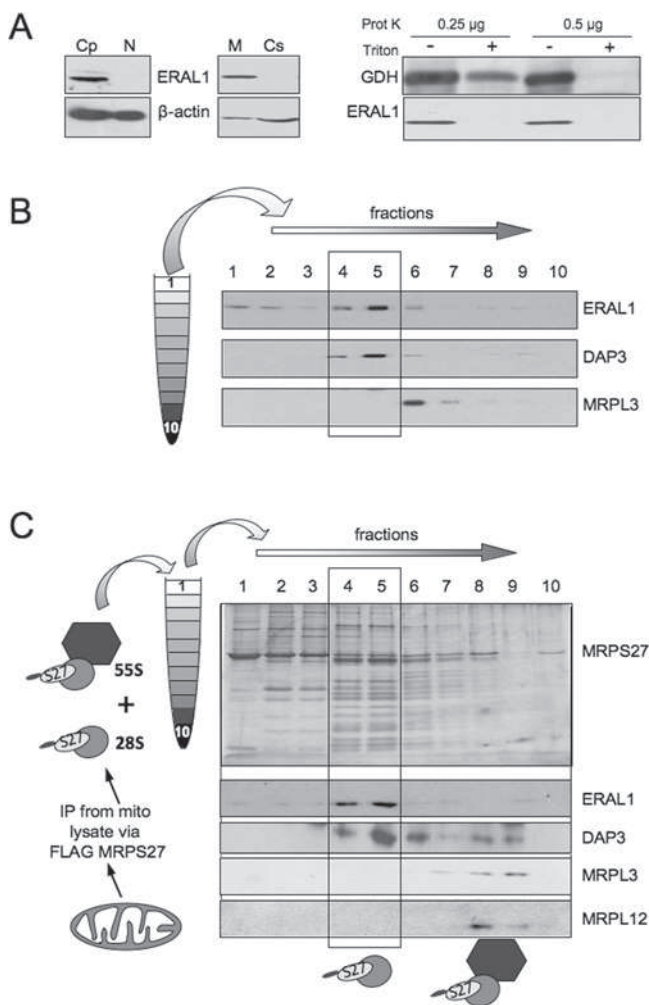


Figure 1 ERAL1 associates with the 28S mt-SSU

(A) Left-hand panel: Western blot analysis, with the indicated antibodies, of HEK-293T cells subfractionated into nuclear (N) or cytoplasmic (Cp) compartments, with the latter fraction further divided into mitochondrial (M) and cytosolic (Cs) fractions. Equivalent volumes of each fraction are loaded. Right-hand panel: mitochondria ($30 \mu\text{g}$) were pretreated with the indicated amounts of proteinase K and solubilized with Triton X-100 or subjected directly to Western blot analysis with the indicated antibodies. (B) HeLa cell lysate (0.7 mg) was separated by isokinetic gradient centrifugation as detailed in the Experimental section, prior to fractionation and Western blot analysis to indicate the position of mitoribosomal subunits (DAP3 for 28S mt-SSU; MRPL3 for 39S mt-LSU). The blot is representative of three independent repeats. (C) Eluted immunoprecipitate from mitochondria of cells expressing MRPS27-FLAG were separated by isokinetic gradient centrifugation and fractions were silver-stained (upper panel) or subjected to Western blotting with the indicated antibodies (lower panels). 28S mt-SSU, grey circle; 39S mt-LSU, black hexagon. Gels are representative of two independent repeats.

density fractions, whereas the majority appeared to co-localize with DAP3, a marker of the mt-SSU (Figure 1B). Separation of the 28S mt-SSU and 39S mt-LSU by isokinetic gradient centrifugation is robust, but the complete 55S monosome is often not detectable. However, by IP of the mitoribosome followed by similar gradient centrifugation, it has been recently reported that the monosome can be detected [20]. To assess whether ERAL1 binds only to the mt-SSU and not the intact monosome, a FLAG-tagged component of the 28S subunit, MRPS27 was inducibly expressed in human HEK-293T cells. Following IP, the bound complexes were eluted and separated through a similar 10–30% isokinetic gradient (Figure 1C). Under these conditions, ERAL1 was mainly visible in fractions 4 and 5, co-migrating with DAP3.

As expected, no 39S subunit is precipitated alone, but DAP3, along with the 39S subunit markers MRPL3 and MRPL12, are visible in fractions 8 and 9, marking the 55S monosome (Figure 1C) with minimal ERAL1 associated.

Depletion causes a loss of *de novo* mt-SSU formation

ERAL1 associates selectively with the mt-SSU, suggesting it may play a role in late 28S assembly. Depletion of ERAL1, would be predicted to result in a reduction of newly formed 28S, while having no effect on 39S mt-LSU formation. Therefore, to investigate the effect of ERAL1 loss on mitoribosome formation, siRNA was used to deplete the protein in cells prior to induction of either a FLAG-tagged component of the 28S (MRPS26) or 39S (ICT1) subunit. Three independent siRNA molecules were able to deplete ERAL1 (Figure 2A). Further experiments were performed with siORF1, directed at the open reading frame, after the likelihood of off-target effects was determined to be minimal (see below). Cells were treated with siORF1 for 24 h prior to induction of FLAG-tagged mitoribosomal protein for a further 2 days. Interestingly, similar signals were apparent in control and ERAL1-depleted samples for protein components of the 28S subunit following ICT1 IP. This suggests that the levels of complete mitoribosome in the control (NT) and ERAL1-depleted (ORF1) cells were similar (Figure 2C). In contrast, markers of both the small and large subunit in the MRPS26 IP were markedly decreased, consistent with a substantial reduction in 28S assembly in the absence of ERAL1 (Figure 2B). Taken together, these results infer that although little nascent 28S subunit is being made after loss of ERAL1, mitoribosome formation is still maintained during the depletion period, presumably due to re-use of 28S mt-SSU that had been assembled prior to ERAL1 depletion. How does ERAL depletion prevent 28S subunit assembly? In bacteria, Era may play a role in maturation of the 16S rRNA, through binding to the larger pre-16S species associated with the 30S ribosomal subunit and by promoting cleavage by various RNases [12]. Human mt-rRNAs are matured from a discrete polycistronic unit, although it is believed that this is mediated by folding of mt-tRNAs that flank both the 12S and 16S mt-rRNAs respectively [21]. To assess the quantity and quality of mitochondrial RNAs, Northern blots were performed after the siRNA treatment of cells (Figure 2D). Depletion of ERAL1 led to a minor increase in the steady-state levels of most mt-mRNAs analysed, with a substantial increase in *MTND2* (mitochondrially encoded NADH dehydrogenase 2) and *MTND3*. Essentially no effect on stability could be measured (Supplementary Figure S1 at <http://www.BiochemJ.org/bj/430/bj4300551add.htm>). The most profound observation, however, was the selective loss of 12S mt-rRNA (Figure 2D, MT-RNR1), consistent with the reduction in 28S mitoribosomal subunit. As 16S mt-rRNA is not depleted (Figure 2D, MT-RNR2) and is produced from the same polycistronic unit, it can be concluded that loss of ERAL1 leads to a rapid and specific degradation of 12S mt-rRNA.

ERAL1 is an RNA chaperone for the 12S mt-rRNA

The degradation of 12S mt-rRNA may be mediated by the lack of mitoribosome assembly; conversely it may be the loss of RNA stability that leads to a mitoribosomal assembly defect. The bacterial Era has been shown to bind 16S rRNA and the human orthologue ERAL1 contains an RNA-binding KH domain. Previously, this KH domain had been shown to be capable of binding RNA, although the target species was unknown [13]. In contrast, the RNA sequence to which the

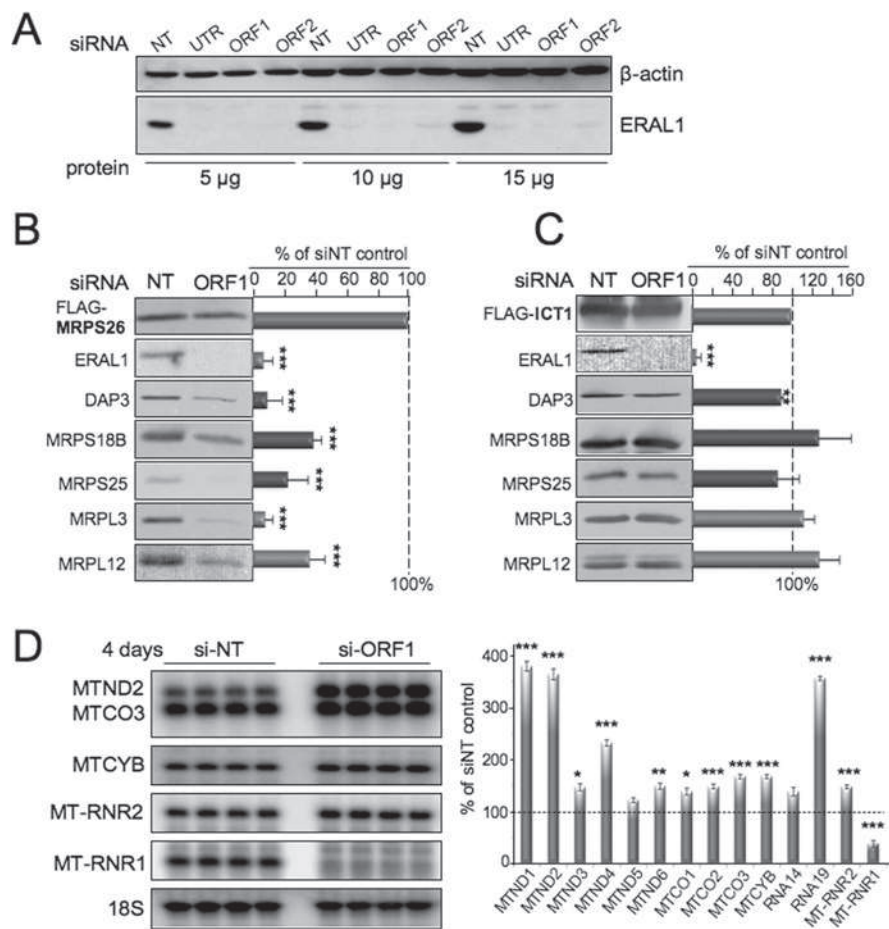


Figure 2 ERAL1 is required for assembly of the 28S small mitoribosomal subunit

(A) Western blot of HEK-293T cell lysate (5, 10 or 15 μ g) pretreated with NT or three independent ERAL1-targeted siRNAs for 3 days and probed with anti-ERAL1 or anti- β -actin antibodies. UTR, siRNA targeting the the 3'-UTR of Eral1; ORF1 and ORF2, siRNAs targeting regions of the open reading frame. In all further siRNA experiments, depletion of ERAL1 was confirmed by Western blotting. (B) Western blot of immunoprecipitate from cells expressing MRPS26-FLAG following 3 days of non-targeting (NT) or ERAL1-depletion (ORF1) siRNA. Position of mitoribosomal subunits are indicated with the markers DAP3, MRPS18B and MRPS25 for the 28S mt-SSU, and MRPL3 and MRPL12 for the 39S mt-LSU. Quantification was performed on three independent experiments. On each occasion, signals were normalized to levels of MRPS26 in the immunoprecipitate. Results are means + S.D. (C) Western blot of immunoprecipitate from cells expressing ICT1-FLAG. Experimental details and data analysis as described for panel (A) ($n = 3$). (D) Northern blot of 4 μ g of RNA isolated from HEK-293T cells treated with si-NT or following ERAL1 depletion (si-ORF1) for 4 days. RNA from four independent experiments is shown. Probes highlight transcripts encoding components of complex I (MTND2), complex III (MTCYB; mitochondrially encoded cytochrome *b*) and complex IV (MTCO3, COX3) as well as both 16S (MT-RNR2) and 12S (MT-RNR1) mt-rRNAs. A probe to human 18S rRNA is shown as a loading and quality control (18S). The quantification is shown for 14 independent transcripts from four repeats. Results are means + S.D. *** $P < 0.001$, ** $P < 0.01$, * $P < 0.05$.

bacterial protein binds has been clearly identified. It is an unstructured nonnucleotide finishing only two nucleotides from the 16S 3' terminus and contains the CCUCC anti-SD sequence that is not present in mammalian 12S mt-rRNA. To identify an RNA-binding footprint on mt-rRNA *in vivo*, we used the CLIP assay that has been established previously for use with cytosolic RNA-binding proteins [19]. Induction of FLAG-tagged ERAL1 was inefficient, resulting in levels similar to endogenous ERAL1 (results not shown). Following induction, cells were UV-irradiated and the bound RNA cleaved by RNase T1 before rescue and identification. As shown in Figure 3(A), 12S mt-rRNA was found in 63% of sequenced clones (31 out of 49), revealing a minimal footprint of 33 nt. This region is close to the 3' terminus of 12S mt-rRNA and spans a stem-loop that has a structural orthologue in bacterial 16S rRNA, but is distinct to the bacterial Era-binding site (Figure 3B). No other mt-rRNA sequence was identified, although several mt-rRNA^{Pro} sequences were recovered (Supplementary Table S1 at <http://www.BiochemJ.org/bj/430/bj4300551add.htm>). The

significance of this is unclear; however, other mitochondrial RNA-binding proteins subjected to CLIP in our laboratory have also shown a similar association with the 3' terminus of mt-rRNA^{Pro} (Mateusz Wydro, unpublished work). The remaining clones contained sequences from *E. coli* 23S rRNA (two clones), human transcripts (three clones) or could not be identified (six clones). We conclude that ERAL1 functions to protect the 12S rRNA by binding at its 3' terminus, but that the position and sequence to which it binds differs from the bacterial protein.

ERAL1 depletion induces cell death prior to mitochondrial translation or respiratory defects

ERAL1 plays an important role in the assembly of the 28S mt-SSU by acting as an RNA chaperone for the 12S mt-rRNA. Depletion with siORF1 resulted in a marked effect on normal (ρ^+) cell growth (Figure 4A), but had no effect on cells that did not require mtDNA expression for growth (ρ^0 ; Supplementary

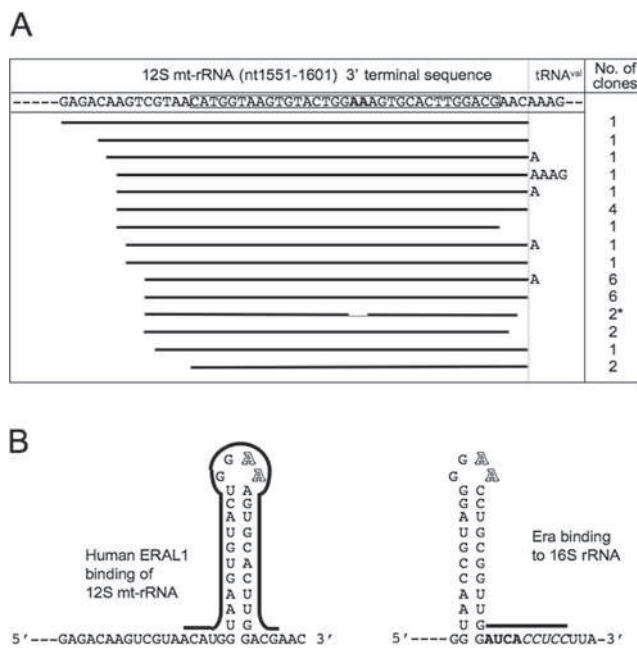


Figure 3 ERAL1 binds *in vivo* to the predicted 3' terminal stem-loop of 12S mt-rRNA

Short RNA species bound by ERAL1 *in vivo* were identified following the CLIP assay as described in the Experimental section. **(A)** The sequence of the 50 nt 3' terminal residues of 12S mt-rDNA, equivalent to nt 1551–1601 of the mitochondrial genome [1] is listed, along with the first four 5' residues of mt-tRNA^{Val}, immediately downstream. The entire insert of each clone is shown as a filled line spanning the corresponding part of the reference sequence, with the number of clones with an identical sequence indicated. The minimal ERAL1-binding site is boxed. The bold AA highlights the dimethylated adenine residues at nt 1582–1583. The sequences of all 31 clones are given in Supplementary Table S1 (at <http://www.BiochemJ.org/bj/430/bj4300551add.htm>). *, two clones were deleted for two A residues of the A triplet at nt 1582–1584. **(B)** The highly conserved 3' terminal stem-loop structure in the mitochondrial 12S (left-hand side) or bacterial 16S (helix 45, right-hand side) [22] are shown, along with the terminal unstructured nucleotides. The minimal 33 nt binding site for ERAL1, along with the delineated nonamer for *Aquifex aeolicus* Era [12] is highlighted as a solid line. The highly conserved AUCA is shown in bold; the anti-S1 region, CCUCC, is italicized. The two dimethylated adenines are shown in outline [23,24].

Figure S2 at <http://www.BiochemJ.org/bj/430/bj4300551add.htm>. A previous report used an inducible knockout technique in a chicken cell line to ablate the *EraL1* gene [14]. This showed that loss of ERAL1 led to cell-cycle arrest and a substantial increase in the proportion of apoptotic cells in the population. We repeated this analysis on HEK-293T cells after 3 days of siRNA treatment and found a similar apoptotic response (with siORF1 35.9 ± 9.5% were apoptotic compared with 0.3 ± 0.4% with NT siRNA, *n* = 4; Supplementary Figure S3 at <http://www.BiochemJ.org/bj/430/bj4300551add.htm>). Intriguingly, however, as shown in Figure 2, although ERAL1 depletion prevented the formation of nascent 28S, it did not reduce the amount of complete mitoribosome during the depletion time course. Consistent with this observation, metabolic labelling experiments showed that mitochondrial protein synthesis in HeLa cells was unaffected even after 4 days of depletion (Figure 4B) and was only partially affected in HEK-293T cells after 3 days of depletion (Figure 4C, left-hand panel). Furthermore, steady-state levels of proteins either directly encoded by mtDNA (COX2) or as markers of stable complexes that incorporate mtDNA-encoded polypeptides (NDUFB8) (Figure 4C, right-hand panel) were unaffected, although a consistent increase in HSP70 was found. These results infer that ERAL1 depletion does not induce

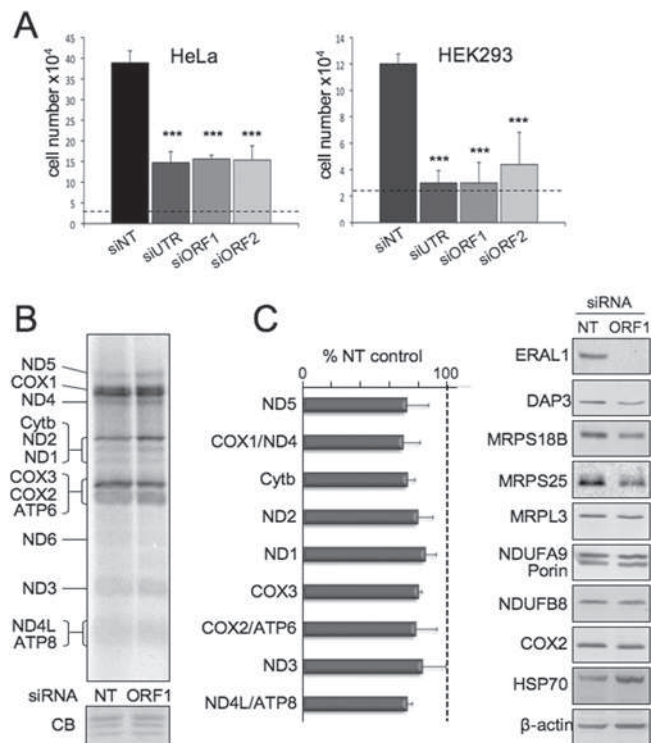


Figure 4 Depletion of ERAL1 leads to apoptosis prior to appreciable loss of mitochondrial protein synthesis

(A) Counts of HEK-293T or HeLa cells were taken after siRNA treatment (3 or 4 days respectively) with an NT control or each of the three independent siRNAs targeted either to the *EraL1* open reading frame (ORF1; ORF2) or to the corresponding 3'-UTR. Counts were performed on three (HeLa) or six (HEK-293T) independent repeats. ****P* < 0.001. **(B)** Metabolic radiolabelling of mitochondrial gene products was performed for 30 min in HeLa cells treated for three days with siRNA (NT or against ERAL1). Aliquots (50 μg) were separated by SDS/PAGE and visualized with a PhosphorImage as described in the Experimental section. Mitochondrial gene products are assigned from [20]. A small section of the gel is shown following exposure, rehydration and Coomassie Blue (CB)-staining to confirm equal loading. ATP8, mitochondrially encoded ATP synthase 8; Cytb, cytochrome *b*; ND, NADH dehydrogenase. **(C)** *De novo* synthesis (left-hand panel) and steady-state levels (right-hand panel) of mt-proteins in HEK-293T cell lysates following 3 days of siRNA treatment (siORF1 or NT control). Quantification of metabolic labelling is presented as a percentage of NT control for each translation product and is from three independent experiments. COX1/ND4, COX2/ATP6 and ND4L/ATP8 were quantified together as they could not confidently be quantified independently. The Western blot analysis visualized mitoribosomal proteins with antibodies as described in the text; markers used are: for complex I, NDUFB8 and NDUFA9; for complex IV, COX2; for the mitochondrial matrix, chaperone HSP70, and for the mitochondrial outer membrane, porin. Results are means ± S.D.

apoptosis merely through the loss of mitochondrial translation products, but may involve a discrete signalling mechanism.

DISCUSSION

ERAL1 is involved in the assembly of the mt-SSU. To date, only one other non-mitoribosomal protein, TFB1M (transcription factor B1, mitochondrial), has been shown to be important for 28S assembly, through its role in dimethylation of the 12S rRNA [25]. Completion of the assembly of the entire mitoribosome has been shown to require proteolytic maturation of MRPL32 by the mAAA protease, which promotes association of the mitoribosome with the inner mitochondrial membrane [26]. Our results show that ERAL1 is a mitochondrial protein whose function is to protect the 12S mt-rRNA on the 28S mitoribosomal subunit during SSU assembly. It therefore has some similar roles to its bacterial counterpart, where Era binding not only protects the

16S rRNA precursor, it also binds in a pocket that precludes the 50S subunit from associating with the 30S subunit. It also prevents mRNA forming the essential SD/anti-SD pairing necessary for protein synthesis initiation [11,12]. No SD motif exists in human mt-mRNA and so no such interaction occurs between the mt-rRNA and mRNA. The molecular mechanism by which the mitoribosome locates the mt-mRNA initiating codon is unclear [27]. Virtually all mt-mRNAs have three or fewer residues of 5'-UTR and for seven of the open reading frames the first 'A' of the initiating codon is the absolute 5' terminal nucleotide [21,28]. Sequence analysis from our CLIP assays reflected physiological binding and demonstrated unequivocally that ERAL1 binds very close to the 3' terminus of the 12S mt-rRNA, covering a sequence predicted to form a terminal stem-loop structure. This small 33 nt footprint includes two adjacent adenosine residues within the loop that are known to be dimethylated by the mitochondrial protein TFB1M in mammals [22,25]. In two of our clones, both of these nucleotides were missing, consistent with methylation of these residues potentially inducing deletions by the reverse transcriptase or indicating their covalent attachment to ERAL1 during UV-irradiation [19]. In cells from mice devoid of TFB1M, levels of the 12S mt-rRNA are dramatically reduced, whereas mt-mRNA levels remain largely unaffected or even increase; both of these results are similar to those noted in human cells depleted of ERAL1. It is tempting to suggest that ERAL1 binding may require adenine dimethylation in the loop. However, in both mice and humans, 12S adenine dimethylation is not absolute. Thus it is possible that ERAL1 has a greater affinity for the dimethylated stem-loop, but can still bind and protect unmethylated species albeit with a weaker affinity.

There is a marked variation between the RNA motif bound by Era in bacteria and ERAL1 in mitochondria. The 12S and bacterial 16S rRNA share sequence and structural similarity in the 3' terminal stem-loop (helix 45 in bacteria), which is clearly identified as the 12S-binding site by our CLIP assays (Figure 3B). The 16S rRNA nucleotides that have been shown by X-ray crystallography to directly interact with the KH domain of *Aquifex aeolicus* Era are nts 1530–1534 (GAUCA) and the anti-SD sequence CCUCC immediately downstream at nts 1535–1539. The AUCA sequence is highly conserved across the domains of life, whereas the anti-SD is present but restricted to prokarya. Strikingly, however, this entire nonanucleotide primary sequence is absent from 12S mt-rRNA (Figure 3B). Therefore although ERAL1 is clearly a mitochondrial orthologue of Era, the RNA bound by the conserved KH domain is completely different. This may reflect the different functions that are required for these orthologues. Binding of Era promotes maturation of pre-16S rRNA by a currently unidentified RNase. Such processing is not required for the 12S equivalent, although binding is clearly needed to protect the 12S mt-rRNA from degradation. Furthermore, it is not clear from our results whether ERAL1 binding to 12S mt-rRNA on the mt-SSU completely precludes association with the mt-LSU as noted on Era binding to bacterial 30S. Clearly, the vast majority of ERAL1 is associated with isolated mt-SSU. However, LC-MS/MS data of complexes immunoprecipitated by ERAL1-FLAG does identify a small number of mt-LSU subunits and this is currently being explored (results not shown).

The protection of mt-mRNAs on ERAL1 depletion and in TFB1M-knockout mice that also prevents assembly of the 28S subunit, suggest that mt-mRNA is not initially associated with the mitoribosome or constituent subunits. Our preliminary results from RNA isolated from gradient fractions suggests that nascent mt-mRNA associates with a separate complex, which increases in mass proportionally with the size of the transcript and that the gradient profile for these mt-mRNAs

remains unchanged in the ERAL1-depleted cells (S. Dennerlein, unpublished work). It is possible that initially after synthesis, mt-mRNA becomes associated with an RNA-binding complex and remains associated until the mt-mRNA is recruited to the mitoribosome for translation. The foundation for such a RNP complex has recently been reported [29]. This RNP contains two generic mitochondrial RNA-binding proteins, LRP130 (130 kDa leucine-rich protein) and SLIRP (stem-loop interacting RNA-binding protein). It is possible and even probable that this complex will associate with other mitochondrial RNA-binding proteins, such as those originally demonstrated in [30].

What is the cause of apoptosis in the ERAL1-depleted cell lines? Clearly, ERAL1 depletion leads to the loss of the newly assembled 28S subunit. However, the depleted lines appear to retain sufficient intact mitoribosomes to allow efficient mitochondrial protein synthesis up to the point when the cells die of apoptosis. This suggests that either the cells synthesize aberrant polypeptides as a function of having to recycle old 28S subunits, or there is an undefined retrograde signal from the mitochondrion to the nucleus that leads to the apoptosis. Polarographic analyses of ERAL1-depleted cells revealed no apparent difference in oxygen utilization or respiratory control ratios (results not shown). Furthermore, we were unable to measure any differences in ROS (reactive oxygen species) production or substantial changes in mitochondrial membrane potential. There have been numerous reports linking mitochondrial ribosomal subunits, such as DAP3, with apoptosis [31,32]. The lack of 28S assembly will result in more freely available polypeptides, but it would appear unlikely that such proteins could be exported from the matrix. Alternatively, perhaps it is possible that lack of SSU assembly leads to accumulation of nascent MRPs, such as DAP3 in the cytosol, leading to apoptosis. This intriguing area is currently being pursued.

Finally, we note that immediately prior to submission of this article, another manuscript was published on the function and localization of ERAL1 [33]. The authors also reported a 28S mitoribosomal association possibly mediated by 12S mt-rRNA-binding and a similar growth phenotype on depletion. However, their siRNA targeted a different sequence to the three siRNAs used in the present study, which we tested for both specific and off-target effects. Unlike the present study, their report indicated that depletion was shown to cause a lowered steady-state level of respiratory complexes, elevated ROS, lowered membrane potential and a substantial reduction in the level of most mtDNA-encoded transcripts. Their observation of this decrease in steady-state levels of mt-mRNA is surprising. It is in contrast with results with TFB1M-knockout mice that exhibit defective mt-SSU formation and in a patient where 12S mt-rRNA is lost as a consequence of a MRPS16 mutation [34], where in neither case is transcript loss noted. Irrespective, we are now able to report that the essential function of ERAL1 is as a 12S mt-rRNA chaperone and the identification of its binding site, *in vivo*.

AUTHOR CONTRIBUTION

Sven Dennerlein carried out the majority of the practical work with the exception that Agata Rozanska performed the CLIP assays and Mateusz Wydro generated the MRPS26 constructs and the HEK-293T cell line with inducible expression of MRPS26. Zofia Chrzanoska-Lightowers and Robert Lightowers provided the funding, intellectual direction and wrote the paper. All authors critically reviewed the paper.

ACKNOWLEDGEMENTS

We thank Joanna Rorbach, for helpful discussions and generating constructs, and Ian Dimmick and Rebecca Stewart (Newcastle University, Flow Cytometry Core Facility), for technical and data analysis advice.

FUNDING

This work was supported by the The Wellcome Trust [grant number 074454/Z/04/Z], the Biotechnology and Biological Sciences Research Council [grant number BB/F011520/1] and the Medical Research Council [grant number G0700718].

REFERENCES

- Anderson, S., Bankier, A. T., Barrell, B. G., De Bruijn, M. H. L., Coulson, A. R., Drouin, J., Eperon, I. C., Nierlich, D. P., Roe, B. A., Sanger, F. et al. (1981) Sequence and organization of the human mitochondrial genome. *Nature* **290**, 457–465
- Sharma, M. R., Koc, E. C., Datta, P. P., Booth, T. M., Spremulli, L. L. and Agrawal, R. K. (2003) Structure of the mammalian mitochondrial ribosome reveals an expanded functional role for its component proteins. *Cell* **115**, 97–108
- O'Brien, T. W. (2003) Properties of human mitochondrial ribosomes. *IUBMB Life* **55**, 505–513
- Magalhaes, P. J., Andreu, A. L. and Schon, E. A. (1998) Evidence for the presence of 5S rRNA in mammalian mitochondria. *Mol. Biol. Cell* **9**, 2375–2382
- Smirnov, A., Tarassov, I., Mager-Heckel, A. M., Letzelter, M., Martin, R. P., Krashennikov, I. A. and Entelis, N. (2008) Two distinct structural elements of 5S rRNA are needed for its import into human mitochondria. *RNA* **14**, 749–759
- Hage, A. E. and Tollervey, D. (2004) A surfeit of factors: why is ribosome assembly so much more complicated in eukaryotes than bacteria? *RNA Biol.* **1**, 10–15
- Britton, R. A. (2009) Role of GTPases in bacterial ribosome assembly. *Annu. Rev. Microbiol.* **63**, 155–176
- Rorbach, J., Richter, R., Wessels, H. J., Wydro, M., Pekalski, M., Farhoud, M., Kuhl, I., Gaisne, M., Bonnefoy, N., Smeitink, J. A. et al. (2008) The human mitochondrial ribosome recycling factor is essential for cell viability. *Nucleic Acids Res.* **36**, 5787–5799
- Ahn, J., March, P. E., Takiff, H. E. and Inouye, M. (1986) A GTP-binding protein of *Escherichia coli* has homology to yeast RAS proteins. *Proc. Natl. Acad. Sci. U.S.A.* **83**, 8849–8853
- Britton, R. A., Powell, B. S., Dasgupta, S., Sun, Q., Margolin, W., Lupski, J. R. and Court, D. L. (1998) Cell cycle arrest in Era GTPase mutants: a potential growth rate-regulated checkpoint in *Escherichia coli*. *Mol. Microbiol.* **27**, 739–750
- Sharma, M. R., Barat, C., Wilson, D. N., Booth, T. M., Kawazoe, M., Hori-Takemoto, C., Shirouzu, M., Yokoyama, S., Fucini, P. and Agrawal, R. K. (2005) Interaction of Era with the 30S ribosomal subunit implications for 30S subunit assembly. *Mol. Cell* **18**, 319–329
- Tu, C., Zhou, X., Tropea, J. E., Austin, B. P., Waugh, D. S., Court, D. L. and Ji, X. (2009) Structure of ERA in complex with the 3' end of 16S rRNA: implications for ribosome biogenesis. *Proc. Natl. Acad. Sci. U.S.A.* **106**, 14843–14848
- Akiyama, T., Gohda, J., Shibata, S., Nomura, Y., Azuma, S., Ohmori, Y., Sugano, S., Arai, H., Yamamoto, T. and Inoue, J. (2001) Mammalian homologue of *E. coli* Ras-like GTPase (ERA) is a possible apoptosis regulator with RNA binding activity. *Genes Cells* **6**, 987–1001
- Gohda, J., Nomura, Y., Suzuki, H., Arai, H., Akiyama, T. and Inoue, J. (2003) Elimination of the vertebrate *Escherichia coli* Ras-like protein homologue leads to cell cycle arrest at G1 phase and apoptosis. *Oncogene* **22**, 1340–1348
- Richter, R., Rorbach, J., Pajak, A., Smith, P. M., Wessels, H. J., Huynen, M. A., Smeitink, J. A., Lightowers, R. N. and Chrzanowska-Lightowers, Z. M. (2010) A functional peptidyl-tRNA hydrolase, ICT1, has been recruited into the human mitochondrial ribosome. *EMBO J.* **29**, 1116–1125
- Soleimanpour-Lichaei, H. R., Kuhl, I., Gaisne, M., Passos, J. F., Wydro, M., Rorbach, J., Temperley, R., Bonnefoy, N., Tate, W., Lightowers, R. and Chrzanowska-Lightowers, Z. (2007) miRF1a is a human mitochondrial translation release factor decoding the major termination codons UAA and UAG. *Mol. Cell* **27**, 745–757
- Ovcharenko, D., Jarvis, R., Hunnicke-Smith, S., Kelnar, K. and Brown, D. (2005) High-throughput RNAi screening *in vitro*: from cell lines to primary cells. *RNA* **11**, 985–993
- Chrzanowska-Lightowers, Z. M., Preiss, T. and Lightowers, R. N. (1994) Inhibition of mitochondrial protein synthesis promotes increased stability of nuclear-encoded respiratory gene transcripts. *J. Biol. Chem.* **269**, 27322–27328
- Ule, J., Jensen, K., Mele, A. and Darnell, R. B. (2005) CLIP: a method for identifying protein–RNA interaction sites in living cells. *Methods* **37**, 376–386
- Chomyn, A. (1996) *In vivo* labeling and analysis of human mitochondrial translation products. *Methods Enzymol.* **264**, 197–211
- Ojala, D., Montoya, J. and Attardi, G. (1981) tRNA punctuation model of RNA processing in human mitochondria. *Nature* **290**, 470–474
- Seidel-Rogol, B. L., McCulloch, V. and Shadel, G. S. (2003) Human mitochondrial transcription factor B1 methylates ribosomal RNA at a conserved stem-loop. *Nat. Genet.* **33**, 23–24
- Van Knippenberg, P. H., Van Kimmenade, J. M. and Heus, H. A. (1984) Phylogeny of the conserved 3' terminal structure of the RNA of small ribosomal subunits. *Nucleic Acids Res.* **12**, 2595–2604
- Brimacombe, R. (1995) The structure of ribosomal RNA: a three-dimensional jigsaw puzzle. *Eur. J. Biochem.* **230**, 365–383
- Metodiev, M. D., Lesko, N., Park, C. B., Camara, Y., Shi, Y., Wibom, R., Hultenby, K., Gustafsson, C. M. and Larsson, N. G. (2009) Methylation of 12S rRNA is necessary for *in vivo* stability of the small subunit of the mammalian mitochondrial ribosome. *Cell Metab.* **9**, 386–397
- Nolden, M., Ehses, S., Koppen, M., Bernacchia, A., Rugarli, E. I. and Langer, T. (2005) The m-AAA protease defective in hereditary spastic paraplegia controls ribosome assembly in mitochondria. *Cell* **123**, 277–289
- Jones, C. N., Wilkinson, K. A., Hung, K. T., Weeks, K. M. and Spremulli, L. L. (2008) Lack of secondary structure characterizes the 5' ends of mammalian mitochondrial mRNAs. *RNA* **14**, 862–871
- Temperley, R. J., Wydro, M., Lightowers, R. N. and Chrzanowska-Lightowers, Z. M. (2010) Human mitochondrial mRNAs-like members of all families, similar but different. *Biochim. Biophys. Acta* **1797**, 1081–1085
- Sasarman, F., Brunel-Guitton, C., Antonicka, H., Wai, T. and Shoubridge, E. A. (2010) LRPPRC and SLIRP interact in a ribonucleoprotein complex that regulates posttranscriptional gene expression in mitochondria. *Mol. Biol. Cell* **21**, 1315–1323
- Koc, E. C. and Spremulli, L. L. (2003) RNA-binding proteins of mammalian mitochondria. *Mitochondrion* **2**, 277–291
- Cavdar Koc, E., Ranasinghe, A., Burkhart, W., Blackburn, K., Koc, H., Moseley, A. and Spremulli, L. L. (2001) A new face on apoptosis: death-associated protein 3 and PDCD9 are mitochondrial ribosomal proteins. *FEBS Lett.* **492**, 166–170
- Kissil, J. L., Deiss, L. P., Bayewitch, M., Raveh, T., Khaspekov, G. and Kimchi, A. (1995) Isolation of DAP3, a novel mediator of interferon-gamma-induced cell death. *J. Biol. Chem.* **270**, 27932–27936
- Uchiumi, T., Ohgaki, K., Yagi, M., Aoki, Y., Sakai, A., Matsumoto, S. and Kang, D. (2010) ERAL1 is associated with mitochondrial ribosome and elimination of ERAL1 leads to mitochondrial dysfunction and growth retardation. *Nucleic Acids Res.*, doi:10.1093/nar/gkq305
- Miller, C., Saada, A., Shaul, N., Shabtai, N., Ben-Shalom, E., Shaag, A., HersHKovitz, E. and Elpeleg, O. (2004) Defective mitochondrial translation caused by a ribosomal protein (MRPS16) mutation. *Ann. Neurol.* **56**, 734–738

Received 21 May 2010/30 June 2010; accepted 6 July 2010

Published as BJ Immediate Publication 6 July 2010, doi:10.1042/BJ20100757

SUPPLEMENTARY ONLINE DATA

Human ERAL1 is a mitochondrial RNA chaperone involved in the assembly of the 28S small mitochondrial ribosomal subunit

Sven DENNERLEIN, Agata ROZANSKA, Mateusz WYDRO¹, Zofia M. A. CHRZANOWSKA-LIGHTOWLERS² and Robert N. LIGHTOWLERS²

Mitochondrial Research Group, Institute for Ageing and Health, Newcastle University, Newcastle upon Tyne NE2 4HH, U.K.

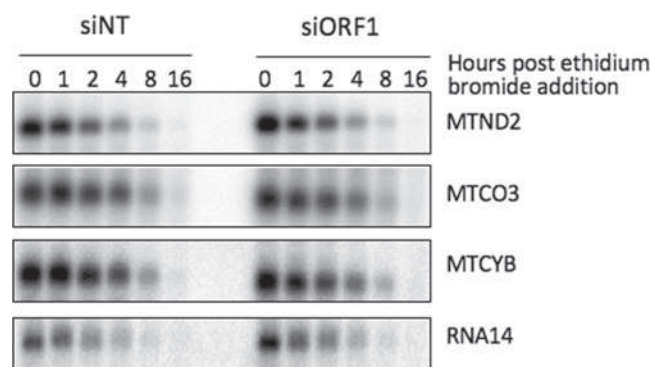


Figure S1 Stability of mitochondrially encoded transcripts is unaffected by loss of ERAL1

HEK-293T cells were transfected with control (siNT) or ERAL1-targeting (siORF1) siRNA for 3 days, after which mitochondrial transcription was inhibited by the addition of ethidium bromide (250 ng/ml). RNA was then isolated at the time points indicated post-addition of transcriptional inhibitor and 4 μ g of each sample was separated through 1.2% agarose under denaturing conditions. Northern blot analysis was performed with random hexamer generated DNA probes to the mitochondrial transcripts indicated. MTCO3, COX3; MTCYB; mitochondrially encoded cytochrome *b*.

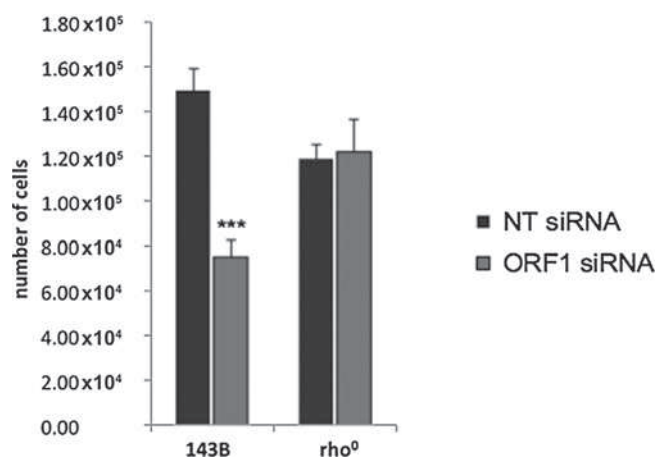


Figure S2 Confirmation that siORF1 that targets ERAL1 lacks off-target effects

End-point cell proliferation was quantified after 3 days of siRNA depletion of ERAL1 in 143B parental and rho⁰ cells with control (NT siRNA) or ERAL1-targeting (ORF1 siRNA). Depletion of ERAL1 with siORF1 showed a significant effect on the proliferation of parental 143B osteosarcoma cells (rho⁺), that contain mtDNA. In contrast, no effect on cell growth was observed in 143B rho⁰ cells (supplemented with 50 μ g/ml uridine) that lack mtDNA and therefore are unaffected as they do not require mtDNA gene expression for growth. Results are means \pm S.D. $P < 0.001$.

¹ Present address: Department of Plant Sciences, University of Cambridge, Downing Site, Downing Street, Cambridge CB2 3EA, U.K.

² Correspondence may be addressed to either of these authors (email z.chrzanowska-lightowlers@ncl.ac.uk or r.n.lightowlers@ncl.ac.uk).

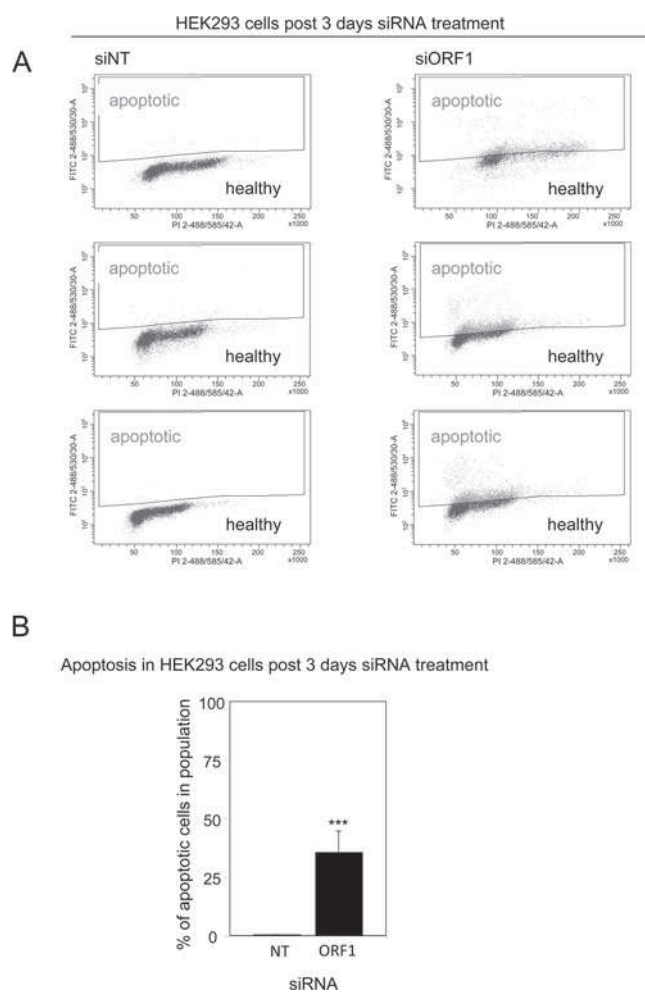


Figure S3 Analysis of apoptosis in HEK-293T cells post-siRNA treatment

HEK-293T cells were treated with control (siNT) or ERAL1-targeting (siORF1) siRNA for 3 days after which the proportion of apoptotic cells was estimated using the APO-Direct kit. **(A)** Representative primary FACS data for the both control and ERAL1-depleted cells. Analyses were performed on independent cultures of siRNA-transfected HEK-293T cells. **(B)** Quantification of the results in **(A)** is presented ($n = 4$) as a percentage of apoptotic cells within the population. Results are means + S.D. $P < 0.001$.

Table S1 Sequences of all 31 short RNA species bound by ERAL1 in the CLIP assay

N, signifies not determined by sequencer; *12S mt-rRNA sequences are portrayed in a linear fashion in Figure 3 in the main paper. TNF, tumour necrosis factor.

CLONE NO.	SEQUENCE	IDENTITY
TCGTAACATGGTAAGTGTACTGGAAAGTGCACCTGGACGAAC 3'term (nt1601)	MT-RNR2 (12S mt-rRNA) *
1.13CGTAACATGGTAAGTGTACTGGAAAGTGCACCTGGACGAAC	
1.14CGTAACATGGTAAGTGTACTGGAAAGTGCACCTGGACGAAC	
1.15CGTAACATGGTAAGTGTACTGGAAAGTGCACCTGGACGAACA	
1.18CGTAACATGGTAAGTGTACTGGAAAGTGCACCTGGACGAACA	
1.21CGTAACATGGTAAGTGTACTGGAAAGTGCACCTGGACGAACA	
1.22AGTCGTAACATGGTAAGTGTACTGGAAAGTGCACCTGGACG	
1.23CGTAACATGGTAAGTGTACTGGAAAGTGCACCTGGACGAAC	
1.24CGTAACATGGTAAGTGTACTGGAAAGTGCACCTGGACGA	
1.25AGTCGTAACATGGTAAGTGTACTGGAAAGTGCACCTGGACGAAC	
2.10AGTCGTAACAT*GTAAGTGTACTGGAAAGTGCACNTGGACGAACAAAG	
2.11GTAACATGGTAAGTGTACTGGAAAGTGCACCTGGACGAAC	
2.13CGTAACATGGTAAGTGTACTGGAAAGTGCACCTGGACGAAC	
2.14AGTCGTAACATGGTAAGTGTACTGGAAAGTGCACCTGGACGAAC	
2.3AGTCGTAACATGGTAAGTGTACTGGAAAGTGCACCTGGACGAAC	
2.6*GGCCGTAACATGGTAAGTGTACTGGAAAGTGCACCTGGACGAACA	
2.7AGTCGTAACATGGTAAGTGTACTGGAAAGTGCACCTGGACGAAC	
2.8CGTAACATGGTAAGTGTACTGGAAAGTGCACCTGGACGAAC	
2.20CATGGTAAGTGTACTGGAAAGTGCACCTGGACGAAC	
2.22CGTAACATGGTAAGTGTACTGGAAAGTGCACCTGGACGAACA	
2.24CGTAACATGGTAAGTGTACTGGAAAGTGCACCTGGACGAAC	
2.25GTCGTAACATGGTAAGTGTACTGGAAAGTGCACCTGGACGAACA	
2.26CGTAACATGGTAAGTGTACTGGAAAGTGCACCTGGACGAAC	
2.28CAAGTCGTAACATGGTAAGTGTACTGGAAAGTGCACCTGGACGAAC	
2.29	GAGACAAGTCGTAACATGGTAAGTGTACTGGAAAGTGCACCTGGACGAAC	
2.31CGTAACATGGTAAGTGTACTGGAAAGTGCACCTGGACGAACA	
2.32CGTAACATGGTAAGTGTACTGGAAAGTGCACCTGGACGAACA	
2.34GTCGTAACATGGTAAGTGTACTGGAAAGTGCACCTGGACGAAC	
2.36CGTAACATGGTAAGTGTACTGGAAAGTGCACCTGGACGAACA	
2.37AGTCGTAACATGGTAAGTGTACTGGAAAGTGCACCTGGACGAACA	
2.38CGTAACATGGTAAGTGTACTGGAAAGTGCACCTGGACGAAC	
2.40CATGGTAAGTGTACTGGAAAGTGCACCTGGACGAAC	
	GGCGCTAATGGTGGAGTTAAAGACTTTTCTCTGACCA	MT-TP (Mt-IRNAPro)
1.16F	.GGCGCTAATGGTGGAGTTAAAGACTTTTCTCTGACCA	
1.17R	GGTGCTAATGGTGGAGTTAAAGACTTTTCTCTGA	
1.26	.GGTGCTAATGGTGGAGTTAAAGACTTTTCTCT	
2.16	.GTGCTAATGGTGGAGTTAAAGACTTTTCTCT	
2.9	.GGTGCTAATGGTGGAGTTAAAGACTTTTCTCTGAC	
2.21	.GGTGCTAATGGTGGAGTTAAAGACTTTTCTCT	
2.27	GGTGCTAATGGTGGAGTTAAAGACTTTTCTCTGACCA	
		E. coli 23S rRNA
1.19	GGGGTCCATCCCGACTTACCAACCGATGCAAACTCCGAATACCAGCAA	
2.18	ATTATACAAAAGGTACGCAGTCACCGAACAAGTCGGCTCCAC	
		KNOWN H. sapiens
2.2	CGCACGGGCTACAACCACGACCAATGATATG	HSP70 protein 8 iso 1
2.6	TCTAGATGCATCTTTAGGAAGCCCTGTGGAAAGGACAAGGACCTGGGACCGGACTGG	TNF receptor family 10B
2.41	AGCGTGTGCCTACCTACGCCGCGAGCGGGTAACCCGTTGAAC	18S rRNA
		UNKNOWN
2.12	AGGAAGTCGATGTTTCAGGCTGTGCTCATGGCTTCGTCGACAATGATG	
2.15	ACACACTGATTCAGGCTCTGGGCTCCTCCCC	
2.17	GTGATAGCCGCTACACTACGACC	
2.23	GGTAGTCTCGGCCCTAAACGATGATCACTAG	
2.35	ATCACTTTCGCATACGGGCTGTACCCGCTATGGCCACACTTCCAGAGTGTCTG	
2.40	TCGTCAGAGAAAACAGCAAGCTGTTCCTGTTACCG	

Received 21 May 2010/30 June 2010; accepted 6 July 2010
 Published as BJ Immediate Publication 6 July 2010, doi:10.1042/BJ20100757

Translation termination in human mitochondrial ribosomes

Ricarda Richter, Aleksandra Pajak, Sven Dennerlein, Agata Rozanska, Robert N. Lightowlers and Zofia M.A. Chrzanowska-Lightowlers¹

Mitochondrial Research Group, Institute for Ageing and Health, Newcastle University Medical School, Framlington Place, Newcastle upon Tyne NE2 4HH, U.K.

Abstract

Mitochondria are ubiquitous and essential organelles for all nucleated cells of higher eukaryotes. They contain their own genome [mtDNA (mitochondrial DNA)], and this autosomally replicating extranuclear DNA encodes a complement of genes whose products are required to couple oxidative phosphorylation. Sequencing of this human mtDNA more than 20 years ago revealed unusual features that included a modified codon usage. Specific deviations from the standard genetic code include recoding of the conventional UGA stop to tryptophan, and, strikingly, the apparent recoding of two arginine triplets (AGA and AGG) to termination signals. This latter reassignment was made because of the absence of cognate mtDNA-encoded tRNAs, and a lack of tRNAs imported from the cytosol. Each of these codons only occurs once and, in both cases, at the very end of an open reading frame. The presence of both AGA and AGG is rarely found in other mammals, and the molecular mechanism that has driven the change from encoding arginine to dictating a translational stop has posed a challenging conundrum. Mitochondria from the majority of other organisms studied use only UAA and UAG, leaving the intriguing question of why human organelles appear to have added the complication of a further two stop codons, AGA and AGG, or have they? In the present review, we report recent data to show that mammalian mitochondria can utilize a -1 frameshift such that only the standard UAA and UAG stop codons are required to terminate the synthesis of all 13 polypeptides.

Introduction

Mitochondria are vital organelles that are present in all nucleated cells of higher eukaryotes. They play critical roles in many processes, including calcium homeostasis, apoptosis, Fe-S cluster formation and oxidative phosphorylation. Mitochondria contain their own genome (mtDNA, where mt is mitochondrial) encoding mt-mRNAs that are translated within the organelle [1]. In humans, these transcripts encode 13 proteins that are all components of the oxidative phosphorylation machinery, in addition to the two mt-rRNAs and 22 mt-tRNAs, which are required for the intramitochondrial translation of the mt-mRNAs. The remaining protein components required for intra-organellar translation and mitochondrial biogenesis are nuclear-encoded and need to be imported from the cytosol. Human mtDNA is a relatively small genome (16569 bp) and is found in many copies per mononucleate cell. A minimal non-coding sequence is present, which contains regions that control the initiation of mtDNA replication and transcription. From these regions, this compact genome is almost fully transcribed from both strands [2]. As a consequence, long polycistronic transcriptional units are generated, which are subsequently processed to separate the mt-rRNA, mt-tRNAs and mt-mRNAs, and are then matured [2,3]. For the mt-tRNAs,

this involves the addition of $-CCA$ to the 3'-terminus of the precursor by the tRNA-nucleotidyltransferase, a protein encoded by *TRNT1* [4]. The 3'-termini of the mt-mRNAs are also matured, but by the addition of a poly(A) tail. This modification appears to be constitutive and is effected by mtPAP, a nuclear-encoded poly(A) polymerase that is specific to mitochondria [5]. In contrast with cytosolic mRNAs, their mitochondrial counterparts lack any modification to the 5'-termini and remain as a simple 5'-PO₄. Another contrasting feature is the relative lack of UTRs (untranslated regions), leaving most ORFs (open reading frames) unflanked. Thus initiation commences at or within three nucleotides of the extreme 5'-termini for all except two of the ORFs, whereas completion of the UAA stop codon is facilitated by the addition of 'A' residues as a consequence of polyadenylation of seven ORFs.

Protein synthesis in the human mitochondrion

Initiation of protein synthesis occurs mainly at AUG codons, but AUA and AUU can also be decoded as initiating methionines [1]. Compared with translation in the eukaryotic cytosol, where there are many IFs (initiation factors) that come together to form the initiation complex, there appears to be a much reduced system in mammalian mitochondria. In the latter, the initiation complex appears to have retained only two homologues: IF2 and IF3 [6,7]. It does appear, however, that mtIF2 may have taken on the functions of

Key words: mitochondrion, protein synthesis, release factor, stop codon, translation termination.

Abbreviations used: IF, initiation factor; mt, mitochondrial; ORF, open reading frame; RF, release factor; RRF, ribosome recycling factor; UTR, untranslated region.

¹To whom correspondence should be addressed (email Z.Chrzanowska-Lightowlers@ncl.ac.uk).

bacterial IF1 [8]. Elongation proceeds along the mt-mRNA facilitated by mtEF-Tu, mtEF-Ts and mtEF-G1 [9–12]. Another major difference lies in the general structure of the mammalian mitochondrial ribosome when compared with the more familiar bacterial 70S and eukaryotic cytosolic 80S counterparts [13]. Rather than a predominance of rRNA, mammalian mitochondrial ribosomes have reduced the RNA component to two shorter rRNA species, 12S and 16S, while concomitantly increasing the number of protein components, thus reversing the conventional ratio to ~70% protein and only ~30% rRNA. As a consequence, the structure is more open and porous with no conventional E-site and with altered sedimentation values of 28S and 39S for the small and large subunits respectively and 55S for the complete monosome [13].

Termination of protein synthesis in human mitochondria

The 55S particle continues protein synthesis until a stop codon is reached and positioned within the A-site. Sequencing of the human mtDNA almost 30 years ago [1] revealed the features mentioned above. This included the reassignment of the standard stop codon UGA as a tryptophan, a not uncommon reassignment in mitochondrial genetic codes. Strikingly, it also indicated the apparent recoding of AGA and AGG as stop signals since each of these triplets is found only once and, in both cases, only at the very end of the ORFs of mitochondrial transcripts *MTCO1* or *MTND6* respectively. The conclusion that these were now stop signals was driven by the fact that the mtDNA does not code for any tRNA that could decode either AGA/AGG triplets and no tRNA has been shown to be imported physiologically into the human organelle [14]. The remaining 11 mitochondrial ORFs terminate in either of the two standard stops, UAA or UAG. The original dilemma was therefore what form of the class I RF (release factor) would be required to promote peptidyl-tRNA hydrolysis at these stop codons? Do human mitochondria follow the bacterial paradigm where two RFs are required to decode the three stop codons (RF1 recognizing UAA/UAG, and RF2 showing specificity for UGA/UAA [15,16]), or do they utilize a single RF more akin to eRF1 (eukaryotic RF1)/aRF1 (archaeal RF1) in the eukaryotic or archaeal cytosol respectively [17,18]? A single mitochondrial RF, however, would have to recognize an unusual and expanded repertoire of four triplets.

Over 12 years ago, bioinformatic mining identified an encouraging candidate for the role of human mtRF1. This protein contained a predicted decoding tripeptide motif (comprising proline and threonine with a variable amino acid between the two and thus designated the 'PXT' motif) which, although divergent, aligned more closely with that of bacterial RF1 than RF2 [19]. The PXT motif in mtRF1 is made up of six amino acids, PEVGLS, rather than just the three, thus differing from the accepted RF1 type PXT consensus in both length and sequence. It was considered that these differences,

when taken with a second sequence variation at the tip of the α -5 helix, could have evolved to allow recognition of this extended repertoire of stop triplets. Subsequent biochemical analysis with mtRF1, however, failed to identify any release activity with any codons. A more recent search for a further candidate identified a protein, mtRF1a, with high overall identity with mtRF1 [20]. Analysis of the codon recognition domains revealed greater similarity to that of the bacterial RF1 homologue and consensus sequences, with PKT as the sequence constituting the tripeptide motif. Activity assays demonstrated that mtRF1a has a specificity for the standard UAA and UAG codons, but fails to recognize AGA/AGG or any other codon tested [20]. Since the *in vitro* assays are performed with 70S bacterial ribosomes, the lack of recognition of AGA/AGG by mtRF1 or mtRF1a could have been the consequence of using a heterologous system, especially in the light of the significant differences between 55S and 70S particles described above. Further bioinformatic searches have now revealed a family of four predicted mitochondrial RFs, with ICT1 and C12orf65 adding to the previously described mtRF1 and mtRF1a. Intriguingly, these two new members, ICT1 and C12orf65, both lack the two regions involved in codon recognition and are therefore unlikely candidates for AGA/AGG recognition [21].

Reanalysis of the two transcripts containing the AGA or AGG codons indicated that each of these triplets is directly preceded by a 'U' nucleotide, which, following procession of the mitochondrial ribosome to the end of the reading frame, would be placed immediately adjacent, in the P-site [1]. Thus, by invoking a single nucleotide shift, a conventional UAG stop signal would be positioned in the A-site. In support of this hypothesis, although 3'-UTRs are unusual in human mt-mRNAs, these are present in both of the transcripts containing in-frame AGA or AGG, and are predicted to form stable secondary structures [22]. Frameshifting on mitochondrial mRNAs is not common and no examples have been identified previously in mammalian mitochondria. Indeed there are only very few examples in mitochondria, all of which thus far are in the +1 direction and occur within the mt-ORFs [23–25]. The frameshifting proposed in human mitochondria would contrast not only with these other mitochondrial examples (as it is in the -1 direction), but also with all standard frameshifts, as it would occur after protein synthesis has been completed. Furthermore, many frameshifts offer an inefficient alternative to readthrough [26], which can be regulated by changes in physiological conditions [27]. In the instance of this human mitochondrial example, there would be no possibility for readthrough, as there is no cognate mt-tRNA for the AGA/AGG triplets. We have been able to test this hypothesis by combining the use of a mitochondrially targeted bacterial A-site-specific endonuclease, mtRelE, together with sequence analysis of the resultant cleaved RNA [22]. These fine mapping data revealed the A-site codon at termination and confirmed that a -1 frameshift does indeed occur. Thus the human mitochondrial translation system only requires the more standard UAG and UAA codons for termination. Moreover, as a consequence,

only a single RF is required, mtRF1a, which has already been characterized to show selectivity and specificity for these two termination signals [20].

Recycling of the human mitochondrial ribosome following translation termination

No orthologue of a class II RF has been identified in human mitochondria, leaving the question of how mtRF1a is removed from the mitoribosome after translation. Recycling of the post-termination complex to release the deacylated mt-tRNA, mt-mRNA and separation of the monosome into the two subunits is effected by the mitochondrial ribosome recycling factor, mtRRF, in conjunction with mt-EF-G2 and mt-IF3 [28–31]. This second elongation factor mt-EF-G2 was characterized recently and appears to play no role in elongation, but co-operates exclusively with mtRRF in the recycling process [29]. The eukaryotic 80S and bacterial 70S ribosomes were believed to employ only a single EF-G for both processes. However, bioinformatic, *in vitro* and *in vivo* data now show that in fact it is not uncommon for bacteria to have separated the elongation and recycling activities and have two EF-G paralogues, as is the case in human mitochondria [32]. Human mtRRF has an N-terminal presequence that targets the protein to the mitochondrion, but this is not cleaved after successful import into the matrix of the organelle, as is the case for many of the nuclear-encoded but mitochondrially destined proteins [28]. Alignment with numerous RRF sequences suggests that the human mtRRF has a 79-amino-acid N-terminal extension that lacks homology with other proteins [28]. Since this is retained in the mature protein, it is tempting to speculate that it may contain as yet uncharacterized functional domains. Investigations are ongoing in our group to determine whether such domains are present and, if so, what their contribution might be to the process of mitoribosomal recycling.

In conclusion, mitochondrial translation and termination, particularly in humans, shares a number of similarities, but also differs in many ways from these processes in bacteria and the eukaryotic cytosol. This is perhaps not surprising, as it has become clear over the last 30 years that the mitochondrial protein synthesis machinery has an essential association with the membrane, reflecting the highly hydrophobic nature of its translation products, exclusively so in mammals. A greater understanding of this process is hampered by a lack of two important factors. First, our inability to manipulate the mitochondrial genome, which means that it is currently not possible to investigate the role of any *cis*-acting elements in mitochondrial translation. Second, although impressive reconstituted protein synthesis systems have been reported, these are essentially hybrid systems and we therefore lack a faithful reconstituted mitochondrial translation system. If either of these two issues can be resolved in the near future, our in-depth understanding of these processes will increase rapidly.

Funding

R.N.L. and Z.M.A.C.-L. thank The Wellcome Trust [grant number 074454/Z/04/Z], Biotechnology and Biological Sciences Research Council [grant number BB/F011520/1] and the Medical Research Council [grant number G0700718] for continuing support.

References

- Anderson, S., Bankier, A.T., Barrell, B.G., De Bruijn, M.H.L., Coulson, A.R., Drouin, J., Eperon, I.C., Nierlich, D.P., Roe, B.A., Sanger, F. et al. (1981) Sequence and organization of the human mitochondrial genome. *Nature* **290**, 457–465
- Falkenberg, M., Larsson, N.G. and Gustafsson, C.M. (2007) DNA replication and transcription in mammalian mitochondria. *Annu. Rev. Biochem.* **76**, 679–699
- Ojala, D., Montoya, J. and Attardi, G. (1981) tRNA punctuation model of RNA processing in human mitochondria. *Nature* **290**, 470–474
- Nagaike, T., Suzuki, T., Tomari, Y., Takemoto-Hori, C., Negayama, F., Watanabe, K. and Ueda, T. (2001) Identification and characterization of mammalian mitochondrial tRNA nucleotidyltransferases. *J. Biol. Chem.* **276**, 40041–40049
- Tomecki, R., Dmochowska, A., Gewartowski, K., Dziembowski, A. and Stepien, P.P. (2004) Identification of a novel human nuclear-encoded mitochondrial poly(A) polymerase. *Nucleic Acids Res.* **32**, 6001–6014
- Grasso, D.G., Christian, B.E., Spencer, A. and Spremulli, L.L. (2007) Overexpression and purification of mammalian mitochondrial translational initiation factor 2 and initiation factor 3. *Methods Enzymol.* **430**, 59–78
- Koc, E.C. and Spremulli, L.L. (2002) Identification of mammalian mitochondrial translational initiation factor 3 and examination of its role in initiation complex formation with natural mRNAs. *J. Biol. Chem.* **277**, 35541–35549
- Gaur, R., Grasso, D., Datta, P.P., Krishna, P.D., Das, G., Spencer, A., Agrawal, R.K., Spremulli, L. and Varshney, U. (2008) A single mammalian mitochondrial translation initiation factor functionally replaces two bacterial factors. *Mol. Cell* **29**, 180–190
- Xin, H., Worliax, V., Burkhart, W. and Spremulli, L.L. (1995) Cloning and expression of mitochondrial translational elongation factor Ts from bovine and human liver. *J. Biol. Chem.* **270**, 17243–17249
- Worliax, V.L., Burkhart, W. and Spremulli, L.L. (1995) Cloning, sequence analysis and expression of mammalian mitochondrial protein synthesis elongation factor Tu. *Biochim. Biophys. Acta* **1264**, 347–356
- Gao, J., Yu, L., Zhang, P., Jiang, J., Chen, J., Peng, J., Wei, Y. and Zhao, S. (2001) Cloning and characterization of human and mouse mitochondrial elongation factor G, *GFM* and *Gfm*, and mapping of *GFM* to human chromosome 3q25.1-q26.2. *Genomics* **74**, 109–114
- Bhargava, K., Templeton, P. and Spremulli, L.L. (2004) Expression and characterization of isoform 1 of human mitochondrial elongation factor G. *Protein Expression Purif.* **37**, 368–376
- O'Brien, T.W. (2003) Properties of human mitochondrial ribosomes. *IUBMB Life* **55**, 505–513
- Kolesnikova, O.A., Entelis, N.S., Jacquin-Becker, C., Goltzene, F., Chrzanoska-Lightowlers, Z.M., Lightowlers, R.N., Martin, R.P. and Tarasov, I. (2004) Nuclear DNA-encoded tRNAs targeted into mitochondria can rescue a mitochondrial DNA mutation associated with the MERRF syndrome in cultured human cells. *Hum. Mol. Genet.* **13**, 2519–2534
- Petry, S., Brodersen, D.E., Murphy, 4th, F.V., Dunham, C.M., Selmer, M., Tarry, M.J., Kelley, A.C. and Ramakrishnan, V. (2005) Crystal structures of the ribosome in complex with release factors RF1 and RF2 bound to a cognate stop codon. *Cell* **123**, 1255–1266
- Laurberg, M., Asahara, H., Korostelev, A., Zhu, J., Trakhanov, S. and Noller, H.F. (2008) Structural basis for translation termination on the 70S ribosome. *Nature* **454**, 852–857
- Song, H., Mugnier, P., Das, A.K., Webb, H.M., Evans, D.R., Tuite, M.F., Hemmings, B.A. and Barford, D. (2000) The crystal structure of human eukaryotic release factor eRF1: mechanism of stop codon recognition and peptidyl-tRNA hydrolysis. *Cell* **100**, 311–321
- Dontsova, M., Frolova, L., Vassilieva, J., Piendl, W., Kisselev, L. and Garber, M. (2000) Translation termination factor aRF1 from the archaeon *Methanococcus jannaschii* is active with eukaryotic ribosomes. *FEBS Lett.* **472**, 213–216

- 19 Zhang, Y. and Spremulli, L.L. (1998) Identification and cloning of human mitochondrial translational release factor 1 and the ribosome recycling factor. *Biochim. Biophys. Acta* **1443**, 245–250
- 20 Soleimanpour-Lichaei, H.R., Kuhl, I., Gaisne, M., Passos, J.F., Wydro, M., Rorbach, J., Temperley, R., Bonnefoy, N., Tate, W., Lightowlers, R. and Chrzanowska-Lightowlers, Z. (2007) mtRF1a is a human mitochondrial translation release factor decoding the major termination codons UAA and UAG. *Mol. Cell* **27**, 745–757
- 21 Richter, R., Rorbach, J., Pajak, A., Smith, P.M., Wessels, H.J., Huynen, M.A., Smeitink, J.A., Lightowlers, R.N. and Chrzanowska-Lightowlers, Z.M. (2010) A functional peptidyl-tRNA hydrolase, ICT1, has been recruited into the human mitochondrial ribosome. *EMBO J.* **29**, 1116–1125
- 22 Temperley, R., Richter, R., Dennerlein, S., Lightowlers, R.N. and Chrzanowska-Lightowlers, Z.M. (2010) Hungry codons promote frameshifting in human mitochondrial ribosomes. *Science* **327**, 301
- 23 Harlid, A., Janke, A. and Arnason, U. (1997) The mtDNA sequence of the ostrich and the divergence between paleognathous and neognathous birds. *Mol. Biol. Evol.* **14**, 754–761
- 24 Mindell, D.P., Sorenson, M.D. and Dimcheff, D.E. (1998) An extra nucleotide is not translated in mitochondrial ND3 of some birds and turtles. *Mol. Biol. Evol.* **15**, 1568–1571
- 25 Russell, R.D. and Beckenbach, A.T. (2008) Recoding of translation in turtle mitochondrial genomes: programmed frameshift mutations and evidence of a modified genetic code. *J. Mol. Evol.* **67**, 682–695
- 26 Dinman, J.D. and Wickner, R.B. (1992) Ribosomal frameshifting efficiency and *gag/gag-pol* ratio are critical for yeast M₁ double-stranded RNA virus propagation. *J. Virol.* **66**, 3669–3676
- 27 Higashi, K., Kashiwagi, K., Taniguchi, S., Terui, Y., Yamamoto, K., Ishihama, A. and Igarashi, K. (2006) Enhancement of +1 frameshift by polyamines during translation of polypeptide release factor 2 in *Escherichia coli*. *J. Biol. Chem.* **281**, 9527–9537
- 28 Rorbach, J., Richter, R., Wessels, H.J., Wydro, M., Pekalski, M., Farhoud, M., Kuhl, I., Gaisne, M., Bonnefoy, N., Smeitink, J.A. et al. (2008) The human mitochondrial ribosome recycling factor is essential for cell viability. *Nucleic Acids Res* **36**, 5787–5799
- 29 Tsuboi, M., Morita, H., Nozaki, Y., Akama, K., Ueda, T., Ito, K., Nierhaus, K.H. and Takeuchi, N. (2009) EF-G2mt is an exclusive recycling factor in mammalian mitochondrial protein synthesis. *Mol. Cell* **35**, 502–510
- 30 Christian, B.E. and Spremulli, L.L. (2009) Evidence for an active role of IF3mt in the initiation of translation in mammalian mitochondria. *Biochemistry* **48**, 3269–3278
- 31 Haque, M.E., Grasso, D. and Spremulli, L.L. (2008) The interaction of mammalian mitochondrial translational initiation factor 3 with ribosomes: evolution of terminal extensions in IF3mt. *Nucleic Acids Res.* **36**, 589–597
- 32 Suematsu, T., Yokobori, S.I., Morita, H., Yoshinari, S., Ueda, T., Kita, K., Takeuchi, N. and Watanabe, Y.I. (2010) A bacterial elongation factor G homologue exclusively functions in ribosome recycling in the spirochaete *Borrelia burgdorferi*. *Mol. Microbiol.* **75**, 1445–1454

Received 26 April 2010
doi:10.1042/BST0381523

Hungry Codons Promote Frameshifting in Human Mitochondrial Ribosomes

Richard Temperley,* Ricarda Richter,* Sven Dennerlein, Robert N. Lightowlers, Zofia M. Chrzanowska-Lightowlers†

Ribosome frameshifting, although rare, must occur in mitochondrial (mt) translation systems with interrupted open reading frames (ORFs) (1), but all human mt-ORFs are unbroken. However, we show that human mitoribosomes do invoke -1 frameshift at the AGA and AGG codons predicted to terminate the two ORFs in *MTCO1* and *MTND6*, respectively. As a consequence, both ORFs terminate in the standard UAG codon, necessitating the use of only a single mitochondrial release factor (2).

Frameshifting could be promoted by (i) paused mitoribosomes on AGA or AGG triplets, because no mt-tRNAs exist that recognize these codons; (ii) upstream “slippery” sequences that are poorly defined in human mt-mRNA; or (iii) a downstream stable secondary structure predicted for both *MTCO1* and *MTND6* (fig. S1) (3). To demonstrate that -1 frameshifting occurs in human mitochondria, we targeted RelE, a bacterial endoribonuclease that specifically cleaves mRNA in the ribosomal A site, to the mitochondrion [mtRelE (4, 5), fig. S2]. This enzyme shows marked sequence preference for standard termination codons UAG and UAA with negligible predicted recognition of AGA and AGG (4). On induction, the majority of *MTCO1* ($68 \pm 1.73\%$, $n = 3$) and *MTCO2* ($70 \pm 1.4\%$, $n = 3$) were intact (Fig. 1A, lanes 1 and 3), ruling out nonspecific transcript degradation by mtRelE. However, mitochondrial translation was reduced for most mt-proteins, including COX1 and ND6 (Fig. 1B). Depletion of the mitochondrial release factor mtRF1a stabilizes transcripts through extended association with the mitoribosome, whereas RelE promotes release of cleaved mRNA from bacterial ribosomes (4). Therefore, mtRelE expression would be predicted to abrogate mitoribosome-mediated protection. mtRF1a depletion in tandem with mtRelE expression does reduce the amounts of full-length mt-transcripts

and markedly so for *MTCO1* (Fig. 1A, lanes 2 and 4), indicating both recognition and cleavage by mtRelE.

Northern analysis could not resolve whether the short 3' untranslated regions (3'UTRs)

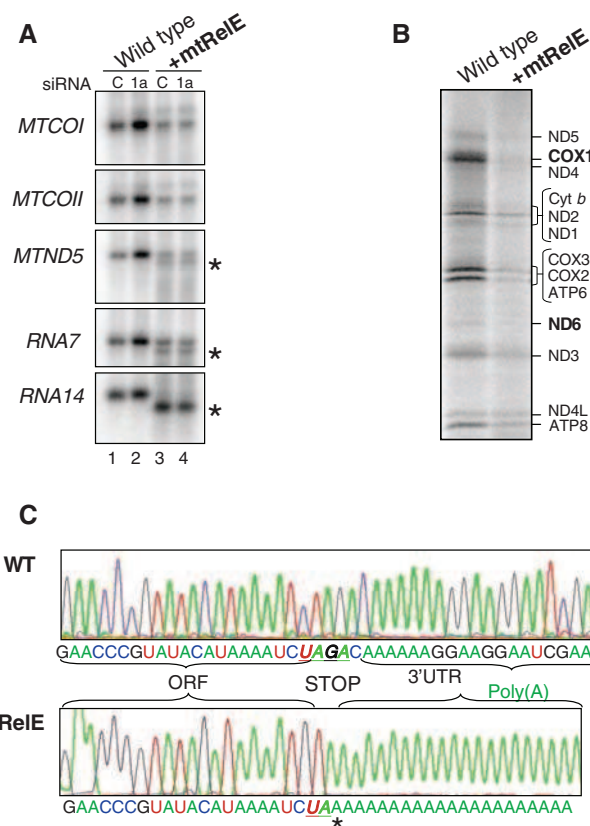


Fig. 1. Expression of mtRelE results in specific cleavage of mt-mRNA stop codons. Cells expressing mtRelE show (A) specific cleavage of mt-mRNA, generating novel products indicated by asterisks in both wild-type (WT) cells and those treated with siRNA to mtRF1a; (B) reduced metabolic labeling of mtDNA encoded gene products; and (C) cleavage of *MTCO1* transcripts specific at the UAG codon (33/35 clones, 2 were common truncated WT sequences) whereas WT cells retained the 3'UTR.

present in *MTCO1* [72 nucleotides (nt)] had been lost post-mtRelE cleavage. *MTND5*, however, possesses a longer 3'UTR (568 nt). On mtRelE induction, a species was detected that is consistent with cleavage at the stop codon and loss of this 3'UTR (Fig. 1A, lanes 3 and 4 indicated by asterisks). Human mtDNA encodes two transcripts with overlapping ORFs, one

containing *MTATP8/6* (*RNA14*) and one *MTND4L/4* (*RNA7*). Cleavage at the stop codon of the upstream ORF would release an RNA with a 5'-truncated downstream ORF. As with *MTND5*, novel species were detected on mtRelE expression. This was particularly apparent for *RNA14*, where *MTATP8* terminates in UAG, a preferred stop codon for RelE (Fig. 1A).

Fine mapping was performed on *MTCO2* and the 5' truncated site of *MTATP6* in the bicistronic *RNA14* (fig. S3). This revealed mtRelE cleavage in the UAG termination codon uniquely between nucleotides 2 and 3 before readenylation. This result therefore allowed us to determine unequivocally whether termination of *MTCO1* occurred at the AGA or UAG codon; AGA termination codon would result in $-AAAAUCUAGA_n$, whereas UAG would produce $-AAAAUCUAA_n$. On sequencing, 10 clones from control cells reflected full-length 3'UTR containing *MTCO1* transcripts; two were truncations in the antisense tRNA^{Ser}, a commonly identified expressed sequence tag. This species was also found in two of the mtRelE samples. However, all the remaining 33 mtRelE clones terminated in $-AAAAUCUA$ followed by readenylation (Fig. 1C), signifying that *MTCO1* terminates at UAG rather than AGA. These data suggest that mtRF1a is sufficient to terminate all 13 human mt-ORFs.

References and Notes

1. R. D. Russell, A. T. Beckenbach, *J. Mol. Evol.* **67**, 682 (2008).
2. H. R. Soleimanpour-Lichaei *et al.*, *Mol. Cell* **27**, 745 (2007).
3. R. F. Gesteland, R. B. Weiss, J. F. Atkins, *Science* **257**, 1640 (1992).
4. K. Pedersen *et al.*, *Cell* **112**, 131 (2003).
5. Materials and methods are available as supporting material on Science Online.
6. This work was supported by the Wellcome Trust (074454/Z/04/Z) and Biotechnology and Biological Sciences Research Council (BB/F011520/1). We thank K. Gerdes for kindly providing the clone and antibodies to bacterial RelE.

Supporting Online Material

www.sciencemag.org/cgi/content/full/327/5963/301/DC1
Materials and Methods
SOM Text
Figs. S1 to S4
Table S1
References and Notes

17 August 2009; accepted 30 November 2009
10.1126/science.1180674

The Mitochondrial Research Group, Institute for Ageing and Health, Newcastle University, Framlington Place, Newcastle upon Tyne NE2 4HH, UK.

*These authors contributed equally to this work.

†To whom correspondence should be addressed. E-mail: Z.Chrzanowska-Lightowlers@ncl.ac.uk